nature microbiology

ARTICLES

https://doi.org/10.1038/s41564-021-00950-8

Identification of Tse8 as a Type VI secretion system toxin from *Pseudomonas aeruginosa* that targets the bacterial transamidosome to inhibit protein synthesis in prey cells

Laura M. Nolan[1,6], Amy K. Cain[2,7,11], Thomas Clamens[1,11], R. Christopher D. Furniss[1,8], Eleni Manoli[1], Maria A. Sainz-Polo[3], Gordon Dougan[2], David Albesa-Jové[3,4,9], Julian Parkhill[2,10], Despoina A. I. Mavridou[1,5]✉ and Alain Filloux[1]✉

The Type VI secretion system (T6SS) is a bacterial nanomachine that delivers toxic effectors to kill competitors or subvert some of their key functions. Here, we use transposon directed insertion-site sequencing to identify T6SS toxins associated with the H1-T6SS, one of the three T6SS machines found in *Pseudomonas aeruginosa*. This approach identified several putative toxin–immunity pairs, including Tse8–Tsi8. Full characterization of this protein pair demonstrated that Tse8 is delivered by the VgrG1a spike complex into prey cells where it targets the transamidosome, a multiprotein complex involved in protein synthesis in bacteria that lack either one, or both, of the asparagine and glutamine transfer RNA synthases. Biochemical characterization of the interactions between Tse8 and the transamidosome components GatA, GatB and GatC suggests that the presence of Tse8 alters the fine-tuned stoichiometry of the transamidosome complex, and in vivo assays demonstrate that Tse8 limits the ability of prey cells to synthesize proteins. These data expand the range of cellular components targeted by the T6SS by identifying a T6SS toxin affecting protein synthesis and validate the use of a transposon directed insertion site sequencing-based global genomics approach to expand the repertoire of T6SS toxins in T6SS-encoding bacteria.

Bacteria rarely exist in a single-species planktonic state and instead form complex polymicrobial structures, called biofilms[1,2]. Within this context, bacteria often compete with other microorganisms to secure space and nutrients. The Type VI secretion system (T6SS) is a Gram-negative bacterial nanomachine that delivers toxins into neighbouring competitors to either kill them or subvert their key functions to attain dominance within a given niche[3–5]. The T6SS is composed of 13 core components, several of which are structurally related to proteins from the T4 bacteriophage tail[6]. The Hcp tube-like structure is capped by a VgrG–PAAR tip complex, or spike, and encapsulated within a TssBC (also known as VipAB) contractile sheath[7–9]. On extension of the sheath within the cytoplasm and subsequent contraction, the spike is thought to facilitate puncturing of the cell membranes of both the producing and target cells, allowing delivery of the attached toxins[8,10]. T6SS toxins have been shown to be secreted in association with the VgrG tip complex, the Hcp tube or as extension domains of the VgrG, PAAR or Hcp proteins[11–14]. Importantly, neighbouring bacterial sister cells are protected from the effects of the toxins by production of cognate immunity proteins, which are usually encoded adjacent to the toxin gene in the genome[15]. The major targets of T6SS toxins identified to date are components of the cell wall, as well as the cell membrane and nucleic acids[16]. These T6SS toxins have mainly been identified by searching in the genomic proximity of known T6SS components, or by detection of toxins in the secretome[11,14,17].

Pseudomonas aeruginosa is a highly antibiotic-resistant Gram-negative pathogen and is ranked second by the World Health Organization in the list of bacteria that require immediate attention. It is equipped with three independent T6SS systems (H1- to H3-T6SS)[18]. In the current study, we used a global genomics-based approach called transposon directed insertion–site sequencing (TraDIS) to identify toxins associated with the *P. aeruginosa* H1-T6SS[19]. A previous study used transposon sequencing, a similar global transposon mutagenesis approach, and confirmed the presence of three T6SS toxin–immunity genes which are located in the vicinity of *vgrG* genes in *Vibrio cholerae*[20]. Our TraDIS approach identified several remote and previously unidentified putative T6SS toxin–immunity pairs. We found that one of the identified toxins, type six exported 8 (Tse8), targets the bacterial transamidosome complex, which is required for protein synthesis in bacteria that lack the asparagine and/or glutamine transfer RNA (tRNA) synthases[21]. This is a previously unidentified target for a T6SS toxin, demonstrating that T6SS toxins can impair bacterial protein synthesis.

[1]MRC Centre for Molecular Bacteriology and Infection (CMBI), Department of Life Sciences, Imperial College London, London, UK. [2]Wellcome Trust Sanger Institute, Wellcome Trust Genome Campus, Cambridge, UK. [3]Structural Biology Unit, CIC bioGUNE, Bizkaia Technology Park, Derio, Spain. [4]IKERBASQUE, Basque Foundation for Science, Bilbao, Spain. [5]Department of Molecular Biosciences, University of Texas at Austin, Austin, TX, USA. [6]Present address: National Heart and Lung Institute, Imperial College London, London, UK. [7]Present address: Department of Molecular Sciences, Macquarie University, Sydney, NSW, Australia. [8]Present address: Science for Life Laboratory, Department of Molecular Biosciences, The Wenner-Gren Institute, Stockholm University, Stockholm, Sweden. [9]Present address: Instituto Biofisika (UPV/EHU, CSIC), Fundación Biofísica Bizkaia/Biofisika Bizkaia Fundazioa (FBB) and Departamento de Bioquímica y Biología Molecular, University of the Basque Country, Leioa, Spain. [10]Present address: Department of Veterinary Medicine, University of Cambridge, Cambridge, UK. [11]These authors contributed equally: Amy K. Cain, Thomas Clamens. ✉e-mail: despoina.mavridou@austin.utexas.edu; a.filloux@imperial.ac.uk

Table 1 | TraDIS allows identification of known and putative previously unidentified H1-T6SS immunity genes

Immunity gene PAK/PA number	Immunity	Toxin	log(fold change)*	Toxin activity/target
PAKAF_RS16410/PA1845	*tsi1*	*tse1*	−2.30	Amidase/peptidoglycan
PAKAF_RS11975/PA2703	*tsi2*	*tse2*	−7.30	Unknown cytoplasmic target
PAKAF_RS07460/PA3485	*tsi3*	*tse3*	−1.28	Muramidase/peptidoglycan
PAKAF_RS11540/PA2775	*tsi4*	*tse4*	−7.30	Unknown periplasmic target
PAKAF_RS12070/PA2683.1	*tsi5*	*tse5*	−7.02	Unknown periplasmic target
PAKAF_RS22000/PA0802	PA0802	PA0801	−6.60	Putative M4 peptidase regulator
PAKAF_RS11515/PA2779	PA2279	PA2778	−5.50	Putative C39 peptidase
PAKAF_RS08570/PA3274	PA3274	PA3272	−4.70	Putative nucleoside triphosphate hydrolase
PAKAF_RS03995/PA4164	*tsi8*	*tse8* (PA4163)	−3.30	Putative amidase

*log(fold change) compared with normalized levels of insertions in T6SS inactive and T6SS active libraries.

TraDIS identifies known and previously unidentified H1-T6SS toxin–immunity pairs. To systematically identify *P. aeruginosa* PAK H1-T6SS associated immunity genes, we generated duplicate high-density insertion transposon mutant libraries consisting of ~2 million mutants in a H1-T6SS active (PAKΔ*retS*) and H1-T6SS inactive (PAKΔ*retS*ΔH1) background. We reasoned that transposon insertions in immunity genes would be tolerated only in the H1-T6SS inactive library, whereas in the H1-T6SS active library, cells lacking an immunity protein would be killed on injection of the cognate toxin from neighbouring sister cells or due to self-intoxication. Each duplicate library was plated separately at high contact density on agar plates and passaged in an overnight incubation step to promote T6SS-mediated killing of mutants with transposon insertions in immunity genes (Extended Data Fig. 1). The genomic DNA of mutants that were not killed in both the H1-T6SS active and inactive libraries were then sequenced separately using a mass-parallel approach, as described previously[22,23] (Extended Data Fig. 1). The relative frequencies of transposon insertion in genes in the H1-T6SS active and inactive libraries revealed a large number of genes that had changes in the relative numbers of transposon insertions. Forty-five genes with a significantly greater number of normalized transposon insertions in the H1-T6SS inactive library background, compared with the H1-T6SS active library background, were identified (Supplementary Table 1) and considered as potential H1-T6SS immunity proteins. Our approach is validated by our ability to identify five (*tsi1*–*tsi5*) of the seven known H1-T6SS immunity genes whose gene products protect against cognate toxins acting in both the cytoplasm and periplasm (Table 1). Our screen was unable to identify *tsi6* because this gene is deleted in our PAKΔ*retS*Δ*H1* strain, thus there is no possibility to assess the relative frequency of transposon insertions in this gene between the two library backgrounds. In the case of *tsi7*, we did not see any difference in the levels of insertions between the two libraries (Supplementary Table 1). It is not clear why this was the case, but we cannot exclude the possibility that one of the uncharacterized proteins encoded by the *vgrG1b* cluster[24] containing the *tse7*–*tsi7* pair, or a gene elsewhere in the genome, can also confer protection against the Tse7 toxin in the absence of Tsi7.

In addition to known H1-T6SS associated immunity genes, our TraDIS approach identified multiple uncharacterized small coding sequences that displayed a decrease in transposon insertions in the H1-T6SS active, compared with the inactive, background (represented by a negative log(fold change)), suggesting a role for these genes in protecting against H1-T6SS-mediated killing (Supplementary Table 1). Upstream of several of these loci were genes encoding proteins with putative enzymatic activity which could be T6SS toxins: PAKAF_04415 (PA0801) encodes a putative M4 peptidase regulator; PAKAF_02303 (PA2778) encodes a putative C39 peptidase domain-containing protein; PAKAF_01709 (PA3272) encodes a putative nucleoside triphosphate hydrolase; and PAKAF_00798 (PA4163) encodes a putative amidase (Table 1 and Extended Data Fig. 2). In the this study, we selected the putative toxin/immunity pair PAKAF_00798/PAKAF_00797 (PA4163/PA4164) for further characterization, and we refer to it as type six exported 8–type six immunity 8 (*tse8*–*tsi8*) in all subsequent sections.

Tse8–Tsi8 is a toxin–immunity pair. To assess the toxic role of Tse8, a strain lacking both *tse8* and the downstream putative immunity gene (*tsi8*) was generated in a PAKΔ*retS* background, yielding PAKΔ*retS*Δ*tsei8*. In this mutant, expression of *tse8* from pMMB67HE with and without a C-terminal haemagglutinin (HA) tag affected growth (Fig. 1a). Furthermore, in a competition assay, this mutant strain carrying a *lacZ* reporter gene (recipient PAKΔ*retS*Δ*tsei8*::*lacZ*) was outcompeted only by donor strains with an active H1-T6SS, that is PAKΔ*retS* or PAKΔ*retS*ΔH2ΔH3 (Fig. 1b). The observed killing of the receiver strain was further demonstrated to be Tse8-dependent in competition assays with a donor lacking Tse8 (Extended Data Fig. 3a). The PAKΔ*retS* strain lacking either *tsei8* or *tse8* could be complemented in a competition assay by expression of *tsei8* from pBBR-MCS5 or *tse8* from pBBR-MCS4 (Extended Data Fig. 3b,c).

The toxicity associated with the H1-T6SS dependent delivery of Tse8 into a sensitive receiver strain could be rescued by expressing the *tsi8* immunity gene from pJN105 in both a competition assay (Fig. 1c) and a growth assay (Fig. 1d), further confirming the protective role of Tsi8. In several cases, T6SS immunity proteins have been shown to interact directly with their cognate toxins[17,25,26]. Here, bacterial two-hybrid (BTH) assays demonstrate that indeed Tse8 interacts strongly with Tsi8 (Fig. 1e). In addition, pull-down experiments using His-tagged Tsi8 (Tsi8–His) as a bait, show direct interaction of the two proteins (Fig. 1f); this interaction is specific to Tsi8 because almost no Tse8 tagged with both an HA and a StrepII tag (Tse8–HA-Strep) elutes from the pull-down beads in the absence of Tsi8–His or in the presence of the non-specific binding control, His-tagged CcmE (CcmE–His) (Fig. 1f).

T6SS toxin delivery frequently relies on a direct interaction between the toxin and components of the T6SS spike[11,14]. BTH assays (Fig. 2a), as well as dot blot assays, revealed that Tse8 interacts strongly with VgrG1a (Fig. 2b). Although the interaction of Tse8 with VgrG1c was significant in the BTH assay (Fig. 2a), no interaction above the non-specific binding control (CcmE–His) was observed in the dot blot assay (Fig. 2b). Finally, no interaction between Tse8 and VgrG1b was observed in BTH (Fig. 2a) or dot blot assays (Fig. 2b).

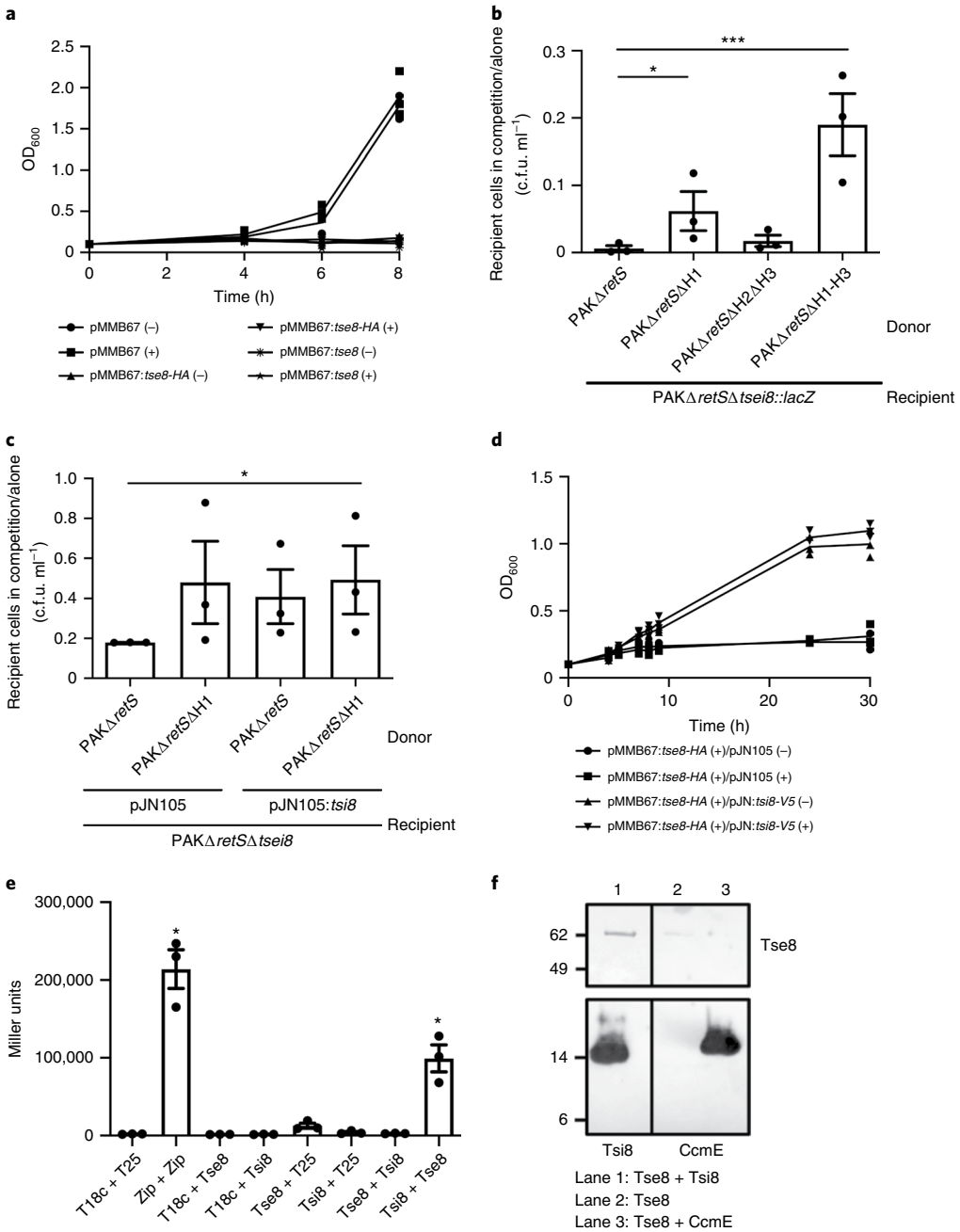

Fig. 1 | Tse8–Tsi8 is a H1-T6SS toxin–immunity pair. a,**b**, Expression of Tse8 (either HA tagged or untagged) in PAKΔ*retS*Δ*tsei8* is toxic when expressed in *trans* from pMMB67HE (–, no induction; +, with induction) (**a**) or when delivered by the H1-T6SS into a recipient strain lacking *tsi8* (**b**). **c**,**d**, Tsi8 can rescue Tse8 toxicity in competition assays with donors PAKΔ*retS* or PAKΔ*retS*Δ*H1* and recipient PAKΔ*retS*Δ*tsei8* expressing either pJN105 or pJN:*tsi8* (**c**) and in growth assays with PAKΔ*retS*Δ*tsei8* expressing pMMB:*tse8* or pJN:*tsi8* (**d**). **e**, BTH assays were used to quantify the level of interaction between Tse8 and Tsi8 with β-galactosidase activity assays performed on the cell lysates of each interaction pair. **f**, Tse8–HA-Strep interacts directly and specifically with Tsi8–His. Proteins were added to His-Tag Dynabeads as indicated. Lane 1: Tsi8–His (as bait) interacts with Tse8–HA-Strep. Lane 2: Tse8–HA-Strep alone does not interact with the Dynabeads. Lane 3: Tse8–HA-Strep does not interact with a different His-tagged bait protein, CcmE. Molecular mass marker positions are indicated on the left in kDa. Black vertical lines indicate where a lane was removed. Statistical analyses were as follows. (**a**) Mean OD_{600} is plotted over time from three independent replicates. (**b**) Mean c.f.u. ml^{-1} of recipient cells in competition/alone are represented from three independent replicates performed in triplicate ($n = 3$); error bars represent ± s.e.m. Two-tailed Student's *t*-test, $^{***}P < 0.001$; $^{*}P < 0.05$; not significant (ns) between PAKΔ*retS* and PAKΔ*retS*ΔH2ΔH3 ($P = 0.436$). (**c**) Mean c.f.u. ml^{-1} of recipient cells in competition/alone are represented from three independent replicates performed in triplicate ($n = 3$); error bars represent ± s.e.m. Two-tailed Student's *t*-test, $^{*}P < 0.05$ for each sample to PAKΔ*retS* and ns between PAKΔ*retS*ΔH1 [pJN105] and PAKΔ*retS* [pJN:*tsi8*] ($P = 0.598$). (**d**) Mean OD_{600} is plotted over time from three independent replicates. (**e**) Mean of three biological replicates performed in triplicate ($n = 3$); error bars represent ± s.e.m. One-way analysis of variance (ANOVA) with Tukey's multiple comparisons post test, $^{*}P < 0.05$ compared with the Miller units for T18c + T25 for Zip + Zip, or compared with Tsi8 + T25 and T18c + Tse8 for Tsi8 + Tse8. (**f**) Representative blot from one independent replicate ($n = 1$).

Overall, the above results demonstrate that Tse8–Tsi8 is an antibacterial toxin–immunity pair associated with the H1-T6SS, and that Tse8 interacts with the VgrG1a-tip to facilitate delivery into target cells.

Tse8 is a predicted amidase family enzyme. Using Phyre2 (ref. [27]) we found that the closest three-dimensional (3D) homologues of Tse8 are the *Stenotrophomonas maltophilia* peptide amidase (Pam)[28] (sequence identity 29%), the *Staphylococcus aureus* Gln-tRNA(Gln) transamidosome subunit A (GatA)[29] (sequence identity 20%), the *P. aeruginosa* Asn-tRNA(Asn) transamidosome subunit A (GatA)[30] (sequence identity 25%), the *Flavobacterium* sp. 6-aminohexanoate cyclic dimer hydrolase (NylA)[31] (sequence identity 24%), the *Bradyrhizobium japonicum* malonamidase E2 (MAE2)[32] (sequence identity 25%), the *Pseudomonas* sp. allophanate hydrolase (AtzF)[33] (sequence identity 30%) and the *Bacterium csbl00001 Aryl Acylamidase* (AAA)[34] (sequence identity 22%). Amino acid sequence analysis indicates that Tse8 contains an amidase signature (AS) domain (Pfam PF01425) (Extended Data Fig. 4). AS sequences are characterized by a stretch rich in glycine and serine residues, as well as a highly conserved Ser–*cis*Ser–Lys catalytic triad[28,29,35–38]. The catalytic Lys is located in the C-terminal end of a conserved β-strand (region 1) (Extended Data Fig. 4), whereas the *cis*Ser is located at the C terminus of region 2 (Extended Data Fig. 4). Finally, the nucleophilic Ser residue is located in a highly conserved short loop of region 3. All these AS signature sequence characteristics (underlined by a dashed line in Extended Data Fig. 4) are present in Tse8 and its closest 3D homologues.

Given that Tse8 possesses the conserved catalytic features of amidase family enzymes (Extended Data Fig. 4), we tested whether it has amidase activity. Tse8 was purified and confirmed to be intact (Extended Data Fig. 5). Subsequently, its capacity to hydrolyse carbon–nitrogen bonds was tested on two molecules, epinecidin-1 and glutamine, which are substrates for Pam from *Stenotrophomonas maltophilia* and GatA of the transamidosome, respectively. The amidase activities of Pam and Tse8 were analysed using mass spectrometry (MS) by monitoring the modifications of epinecidin-1 in the presence and absence of the tested proteins and of the small nucleophile hydroxylamine (Extended Data Fig. 6). Although the C terminus of epinecidin-1 was deaminidated in the presence of Pam (Extended Data Fig. 6b), it remained amidated in the presence of Tse8, suggesting that Tse8 has no amidase activity on this substrate (Extended Data Figs. 6 and 7). The amidase activity of Tse8 was also tested on the GatA substrate glutamine (Extended Data Fig. 8) and no modification was detected using MS (Extended Data Fig. 8b). In addition, whole-cell glutaminase assays were performed and the amidase activity of *Escherichia coli* whole-cell lysates expressing GatA or Tse8 on L-glutamine was determined by monitoring the accumulation of nicotinamide adenine dinucleotide phosphate (NADPH). These experiments demonstrated that, whereas GatA expressed from plasmid pET41a had a significant amidase activity, whole cells expressing Tse8 from the same vector produced a level of NADPH that was not significantly different from the empty vector-carrying control strain (Extended Data Fig. 8c). Overall, these data demonstrate that the substrates for Pam and GatA are not substrates for Tse8, suggesting that Tse8 is highly specific or unlikely to utilize amidase activity to elicit toxicity.

To assess whether Tse8 toxicity is mediated through amidase activity in vivo, we replaced the *tse8* gene on the chromosome with an allele encoding a putative catalytic site mutant of Tse8 with a Ser186Ala (S186A) substitution. This conserved Ser186 residue (Extended Data Fig. 4) acts as the catalytic nucleophile in homologous amidases and is necessary for enzymatic function[39]. PAKΔ*retS* and PAKΔ*retS*ΔH1 donor strains encoding either wild-type Tse8 or Tse8S186A were competed against the recipient strain PAKΔ*retS*Δ*tsei8::lacZ*. This showed that there was no difference in the recovered number of colony-forming units per millilitre (c.f.u. ml^{-1}) of the recipient when the attacking strain delivered either wild-type Tse8 or Tse8S186A (Fig. 2c), further suggesting that Tse8 does not utilize amidase activity to elicit toxicity in vivo.

Tse8 elicits toxicity by interacting with the bacterial amidotransferase complex. Because Tse8 toxicity does not appear to depend on it having amidase activity (Fig. 2c), we hypothesized that Tse8 could instead be eliciting toxicity by competing with a functional amidase either within the cell or within a complex in the cell. Two 3D homologues of Tse8 are the A subunit of the *S. aureus* Gln-tRNA(Gln) transamidosome and the *P. aeruginosa* Asn-tRNA(Asn) transamidosome. Both of these proteins are the A subunit of transamidosome complexes, which are used by bacteria that lack the cognate tRNA synthases for asparagine and/or glutamine[21]. These bacteria utilize a two-step pathway instead, whereby a non-discriminating tRNA synthase generates a misacetylated aspartate- or glutamate-loaded tRNA that is then transaminated by the heterotrimeric amidotransferase enzyme GatCAB, within the transamidosome complex, to leave asparagine or glutamine correctly loaded onto their cognate tRNA. Given that not all bacteria rely on the transamidosome for protein synthesis, we reasoned that if Tse8 toxicity is directed at this enzymatic complex, then expression of Tse8 should be toxic only in bacteria that use the transamidosome. *P. aeruginosa* relies on the transamidosome for Asn-tRNA synthesis[40] and we see a growth defect when Tse8 is expressed from a plasmid or delivered into a strain lacking Tsi8 (Fig. 1a–d). *Agrobacterium tumefaciens* lacks both Asn-tRNA and Gln-tRNA synthases and generates these cognate tRNAs through the transamidosome (Supplementary Table 4), whereas *E. coli* possesses both the Asn- and Gln-tRNA synthases and does not have a transamidosome complex (Supplementary Table 4). The effect of Tse8 expression was examined for both *A. tumefaciens* and *E. coli*. A growth defect was observed for *A. tumefaciens that* could be rescued by coexpression of Tsi8 (Fig. 3a), but no growth defect was observed for *E. coli* (Fig. 3b) despite Tse8 expression at high levels from pET28a (Fig. 3c). Taken together, these data suggest that Tse8 toxicity depends on the presence of the transamidosome.

We generated a structural homology model of Tse8 based on the solved *S. aureus* GatA 3D structure (PDB: 2F2A). By overlaying this model with the A subunit of the *P. aeruginosa* transamidosome structure (PDB: 4WJ3) (Extended Data Fig. 9a), we found that Tse8 shares a high level of structural similarity with the A subunit of the complex. Further, comparison of the homologous residues within the substrate-binding pockets of *Sa*GatA and *Pa*Tse8 revealed that although the catalytic triad residues are conserved, the substrate-binding residues (Tyr309, Arg358 and Asp425 in *Sa*GatA)[29] are not (Extended Data Fig. 9b), supporting our data and hypothesis that Tse8 does not have the same substrate as GatA (Extended Data Fig. 8). While this manuscript was in preparation, a structure for Tse8 was published (RDB: 6TE4)[41] that agrees with the overall conclusions from our homology modelling data.

Given the high level of predicted structural similarity between GatA and Tse8 we hypothesized that Tse8 may be able to interact with the transamidosome and could be eliciting toxicity by altering the functionality of this complex. The most likely scenario was that Tse8 replaces GatA, thus rendering the GatCAB complex inactive. To investigate this, we performed a pull-down experiment using purified proteins. GatCAB was purified as a complex using a Ni-affinity column through His-tagged GatB (His–GatB); GatA and GatC also had tags which were appropriate for their detection by western blot (GatA–V5 and GatC–HA). Tse8 was purified separately through a StrepII tag (Tse8–HA-Strep). GatCAB was pulled down in the presence and absence of a 15-fold molar excess of Tse8–HA-Strep via His–GatB on His-Tag Dynabeads. Tse8 was found to copurify with GatCAB (lane 2, Fig. 3d). This interaction is specific

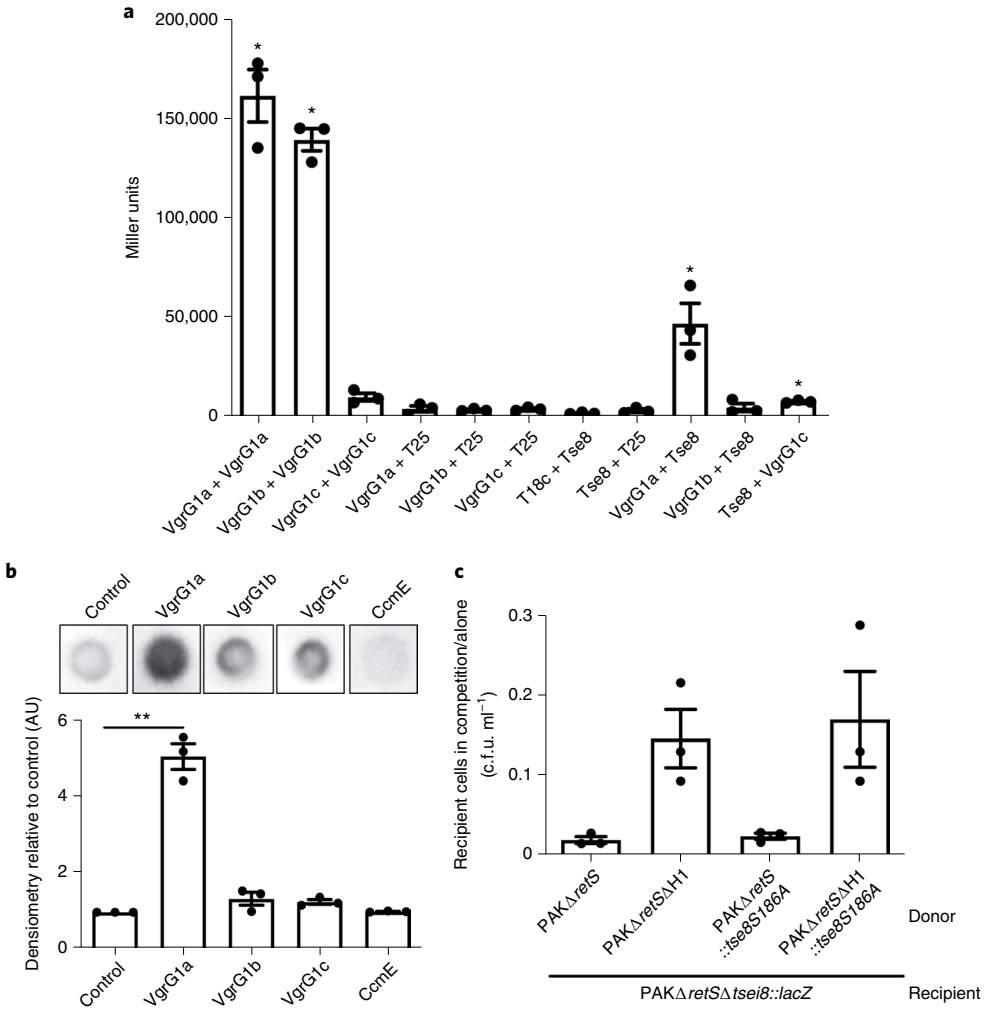

Fig. 2 | Tse8 interacts with VgrG1a and does not require putative catalytic residue for toxicity. a, BTH assays were used to quantify the level of interaction between Tse8 and VgrGs with β-galactosidase activity assays performed on the cell lysates of each interaction pair. **b**, Tse8 interacts with VgrG1a in dot blot assays (upper). Densitometry quantifications of Tse8 interactions with respective partners (lower). CcmE–His is used as a non-specific binding control. **c**, Tse8 toxicity is not dependent on the conserved putative catalytic residue S186. Competition assays were performed with donors PAKΔ*retS*, PAKΔ*retS*ΔH1, PAKΔ*retS*::*tse8S186A* or PAKΔ*retS*ΔH1::*tse8S186A* and recipient PAKΔ*retS*Δ*tsei8*::*lacZ*. Statistical analyses were as follows. (**a**) Mean of three biological replicates performed in triplicate ($n = 3$); error bars represent ± s.e.m. One-way ANOVA with Tukey's multiple comparisons post test, $^{*}P < 0.05$ compared to the Miller units for each of VgrG1a, VgrG1b, VgrG1c and Tse8 with the respective T18c or T25 partner. (**b**) Densitometry measurements normalized to the control and represented as the mean from three independent replicates ($n = 3$); error bars represent ± s.e.m. Two-tailed Student's *t*-test, $^{**}P < 0.005$ compared with control; ns between control and VgrG1b ($P = 0.169$), VgrG1c ($P = 0.067$) and CcmE ($P = 0.159$). (**c**) Mean c.f.u. ml^{-1} of recovered recipient are represented from three independent replicates performed in triplicate ($n = 3$); error bars represent ± s.e.m. Two-tailed Student's *t*-test, $P < 0.05$ for PAKΔ*retS* compared with PAKΔ*retS*ΔH1 and PAKΔ*retS*ΔH1::*tse8S186A*; ns between PAKΔ*retS* and PAKΔ*retS*::*tse8S186A* ($P = 0.226$).

to GatCAB, because minimal amounts of Tse8–HA-Strep elute from the pull-down beads in the absence of the transamidosome or in the presence of the non-specific binding control (CcmE–His) (Fig. 3d). However, even though a large molar excess of Tse8 was used in our pull-down experiment, the amount of GatA detected in the GatCAB complex remained largely unaffected (lane 2, Fig. 3d) excluding the possibility that Tse8 displaces GatA.

Another possibility was that Tse8 interacts with transamidosome components as the GatCAB complex assembles and that this interaction disrupts transamidosome function. To test this hypothesis, we purified GatBC as a complex using a Ni-affinity column through His–GatB and used this complex in pull-down experiments with cell lysates containing GatA and Tse8; GatA, GatC and Tse8 also had tags that were appropriate for their detection by western blot (GatA–V5, GatC–HA and Tse8–HA-Strep). We found that that the presence of Tse8, rather than inhibiting the binding of GatA to GatBC as we initially hypothesized, promotes it (lane 2, Fig. 3e), leading to a drastic accumulation of GatA on the GatBC complex (Fig. 3f). This GatA accumulation is specific to the presence of Tse8 and GatBC, because no GatA elutes from the pull-down beads in the absence of these proteins or in the presence of the non-specific binding control (CcmE–His) (Fig. 3e). The fact that we did not observe GatA accumulation on Tse8 exposure in our pull-down using intact GatCAB (Fig. 3d), suggests that Tse8 is more effective when it acts on transamidosome components during the assembly of this complex. The structure of the *P. aeruginosa* GatCAB transamidosome reveals it to be a symmetric complex comprising an aspartyl-tRNA synthase (ND-AspRS), GatCAB and tRNA^{Asn} in a defined 2:2:2 stoichiometry[30] (as represented in Extended Data Fig. 9a). The function of this complex relies on large conformational changes between the ND-AspRS and the GatCAB components

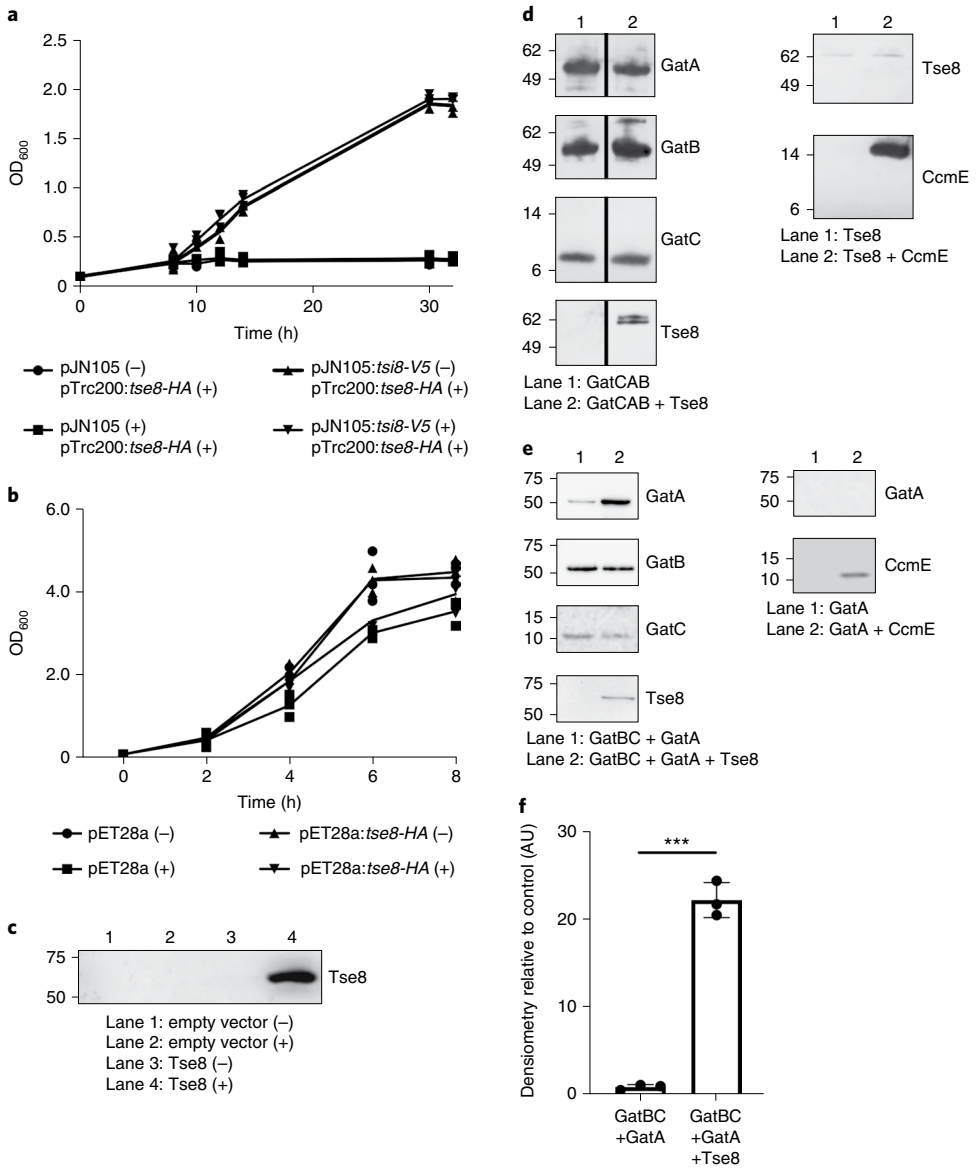

Fig. 3 | Tse8 targets the transamidosome. a–c, Tse8 is only toxic in bacteria that rely on the transamidosome for protein synthesis. Expression of Tse8 in *A. tumefaciens* is toxic but can be rescued by coexpression of Tsi8 (–, no induction; +, with induction) (**a**). Expression of Tse8 in *E. coli* is not toxic (–, no induction; +, with induction) (**b**), despite Tse8 being expressed (**c**). **d**,**e**, Proteins were added to His-Tag Dynabeads as indicated. **d**, (Left) Lane 1: His-GatB (as bait) interacts with GatC–HA and GatA–V5. Lane 2: Tse8–HA-Strep interacts with the GatCAB complex, but does not displace GatA–V5, even at a 15-fold molar excess. (Right) Lane 1: Tse8–HA-Strep alone does not interact with the Dynabeads. Lane 2: Tse8–HA-Strep does not interact with a different His-tagged bait protein, CcmE. **e**, (Left) Lane 1: His-GatB (as bait) interacts with GatC–HA and GatA–V5. Lane 2: the presence of Tse8–HA-Strep leads to a drastic increase of the amount of GatA–V5 interacting with His-GatB and GatC–HA. (Right) Lane 1: GatA–V5 alone does not interact with the Dynabeads. Lane 2: GatA–V5 does not interact with a different His-tagged bait protein, CcmE. **f**, Quantification of the amount of GatA–V5 bound to His-GatB and GatC–HA in the presence or absence of Tse8–HA-Strep by densitometry. (**c**–**e**) Molecular mass marker positions are indicated on the left in kDa. Statistical analyses were as follows. (**a**,**b**) Mean OD_{600} is plotted over time from three independent replicates. (**c**) Representative blot from three independent replicates ($n = 3$). (**d**) Representative blots from one independent replicate ($n = 1$). (**e**) Representative blots from three independent replicates ($n = 3$) for the left panel and one independent replicate ($n = 1$) for the right panel. (**f**) Mean densitometry from three independent replicates ($n = 3$); error bars represent ± s.e.m. Two-tailed Student's *t*-test, $^{***}P < 0.001$ for GatBC+GatA compared with GatBC+GatA+Tse8.

that are fine-tuned to accommodate movement of the $tRNA^{Asn}$ between the domains of the transamidosome super-complex[30]. As such, additional Tse8 and GatA domains attached to the optimal transamidosome complex structure would likely inhibit transamidosome function by obstructing the communication between the ND-AspRS, GatCAB and the $tRNA^{Asn}$. This in turn would result in a decrease in the production of Asn-$tRNA^{Asn}$, ultimately impairing protein synthesis.

To further support our data suggesting that Tse8 exerts its toxicity by impairing protein synthesis through inhibition of the transamidosome, we hypothesized that if we were able to override the need for transamidosome function by providing the bacterium with the tRNA synthase it lacked, we would be able to rescue the observed growth defect when Tse8 is either expressed from a plasmid (Fig. 1a,d) or delivered by an attacker (Fig. 1b,c). *P. aeruginosa* only lacks the asparagine tRNA synthase[40] (Supplementary Table 4),

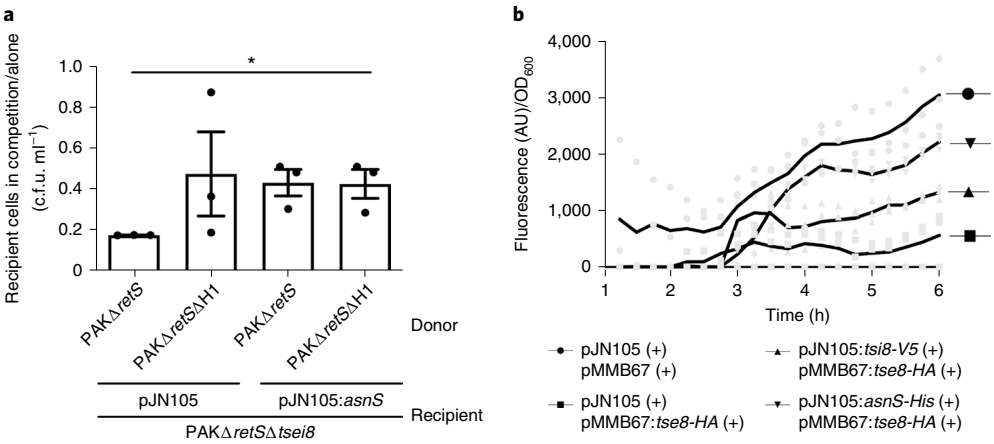

Fig. 4 | Tse8 impacts on protein synthesis in vivo. a, Asn-tRNA synthase (*asnS*) can rescue Tse8 toxicity. Competition assays were performed with donors PAKΔ*retS* or PAKΔ*retS*Δ*H1* and recipient PAKΔ*retS*Δ*tsei8* expressing either pJN105 or pJN:*asnS*. **b**, Cells expressing Tse8 produce less sfGfp/total cells compared with an empty vector control. This effect can be rescued by expression of Tsi8 or AsnS. sfGfp levels normalized to total cells (measured by OD_{600}) were monitored over time in PAKΔ*retS*Δ*tsei8* with sfGFP expressed from the vacant Tn*7* chromosomal site in cells containing the indicated plasmids (+, with induction). Statistical analyses were as follows. (**a**) Mean c.f.u. ml^{-1} of recipient cells in competition/alone are represented from three independent replicates performed in triplicate ($n = 3$); error bars represent ± s.e.m. Two-tailed Student's *t*-test, $^*P < 0.05$; ns for PAKΔ*retS*ΔH1 [pJN105] versus PAKΔ*retS* [pJN:*asnS*] ($P = 0.687$) or versus PAKΔ*retS*ΔH1 [pJN:*asnS*] ($P = 0.631$). (**b**) Mean fluorescence (AU)/OD_{600} is plotted over time from three independent replicates performed in eight technical replicates ($n = 3$).

thus in this case, Tse8 toxicity should be rescued by simply providing the cell with this tRNA synthase. To investigate this possibility, the Asn-tRNA synthase (*asnS*) from *E. coli* was expressed in PAKΔ*retS*Δ*tsei8* from pJN105, and the strain competed against PAKΔ*retS* and PAKΔ*retS*Δ*H1*. Expression of AsnS was able to rescue Tse8 toxicity (Fig. 4a) to the same extent as expression of the cognate immunity protein, Tsi8 (Fig. 1c). Furthermore, to directly test the effect of Tse8 expression on protein synthesis in vivo we expressed superfolder Gfp (sfGfp) from the Tn*7* site of the *P. aeruginosa* chromosome in a Tse8-sensitive strain (PAKΔ*retS*Δ*tsei8*) that also expressed Tse8 or harboured the empty pMMB67HE vector. We found that the strain expressing Tse8 produces less sfGfp compared with the empty vector control (sfGfp signal was normalized to the optical density (OD) at 600 nm; Fig. 4b), and that this effect is specific to Tse8, because the decrease in sfGfp/total cells level in the presence of Tse8 could be rescued by coexpression of Tsi8 (Fig. 4b). Finally, coexpression of Tse8 with *E. coli* AsnS, also rescues the production of sfGfp/total cells (Fig. 4b), demonstrating that the decrease in fluorescent signal observed in the presence of Tse8 alone originates from the specific interaction of Tse8 with its target, the transamidosome complex. Together these data demonstrate that strains containing Tse8 are less able to produce sfGfp, which, in turn, indicates that protein synthesis is inhibited by this T6SS toxin.

Discussion

In the current study we demonstrate that our global genomic approach can be used to identify T6SS toxin–immunity pairs associated with the H1-T6SS of *P. aeruginosa*. Our approach not only confirmed previously characterized *P. aeruginosa* T6SS toxin–immunity pairs, but also revealed several previously unidentified putative toxin–immunity pairs, including Tse8–Tsi8, which would probably not have been found using targeted approaches or bioinformatics. Characterization of the Tse8–Tsi8 pair revealed that Tsi8 is the cognate immunity protein for the Tse8 toxin, and that Tse8 interacts with VgrG1a, hence it is likely delivered into target cells via the VgrG1a-tip complex.

Tse8 was also found to interact with GatCAB of the bacterial transamidosome complex, which is required for protein synthesis in certain bacteria that lack one or both of the asparagine or glutamine tRNA synthases[21]. Our pull-down data (Fig. 3e,f) demonstrate that Tse8 interaction with transamidosome components leads to accumulation of GatA on GatBC, resulting in an amidotransferase complex with altered stoichiometry. Transamidosome function depends on a series of interactions between its ND-AspRS, GatCAB and the $tRNA^{Asn}$ components. These interactions are, in turn, reliant on the optimal architecture of the transamidosome that allows for extensive conformational changes to take place in order for the $tRNA^{Asn}$ to efficiently move between the domains of the super-complex[30]. It would be expected that Tse8-mediated precipitation of several additional GatA molecules on this complex will impact on its fine-tuned architecture, resulting in functional deficits. According to our pull-down data, very little Tse8 is pulled with GatBC (Fig. 3e; all blots in this figure have been exposed for the same amount of time using comparable commercial antibodies). This small amount of toxin is sufficient to nucleate the accumulation of GatA in substantial amounts (Fig. 3f) and impair transamidosome function. Overall, this is in agreement with the logistics of Tse8 being delivered through the VgrG1a-tip complex, whereby only a maximum of three molecules of toxin can be delivered per T6SS firing event through VgrG. Based on this data, we propose that in bacteria where the transamidosome is essential (that is, in bacteria lacking one or both of the Asn- or Gln-tRNA synthases), activity of Tse8 results in reduced fitness due to decreased levels of protein synthesis. In agreement with this, Tse8 toxicity can be rescued if the transamidosome function is bypassed on provision of the transamidosome-independent tRNA synthase lacked by the bacterium (that is, AsnS for *P. aeruginosa*; Fig. 4a,b).

Future work, focusing on further characterization of the specifics of the Tse8–GatCAB interaction, could point to ways of inhibiting the transamidosome and may provide a basis for the development of antibacterial agents against this target. Such agents might be useful in inhibiting the growth of important pathogens that rely on the transamidosome, without affecting the viability of commensal bacteria that produce their proteins without depending on this pathway. Moreover, investigation of the other putative toxins detected in this study could also open up new therapeutic avenues; elucidation of the substrates of these putative toxins could

offer insights into pathways that are naturally validated antibacterial targets against *P. aeruginosa*. Looking beyond the T6SS of *P. aeruginosa*, there are many Gram-negative bacteria that infect human and animal hosts, or are plant pathogens or plant-associated organisms and possess at least one, if not multiple T6SSs clusters[42,43–45]. Furthermore, in several cases it has been demonstrated that distinct T6SS machines deliver a specific subset of toxins into target cells, often under very specific conditions[9,12,16], suggesting that toxins are not only bacteria specific, but potentially even niche specific. Given this diversity, we predict that our TraDIS approach could be useful for drastically expanding the repertoire of known T6SS toxins across a range of bacteria and ecologically or clinically relevant growth environments.

Methods

Bacterial strains, plasmids and growth conditions. Bacterial strains and plasmids used in this study are reported in Supplementary Table 2. *P. aeruginosa* PAK was used for TraDIS library generation and subsequent assays using mutant strains generated by allelic exchange mutagenesis as described previously[46,47]. *P. aeruginosa* strains were grown in tryptone soy broth (TSB), lysogeny broth (LB) or M9 or MOPS minimal media (with indicated supplements), supplemented with antibiotics as appropriate (streptomycin 2,000 μg ml^{-1}, carbenicillin 100 μg ml^{-1}, gentamicin 50 μg ml^{-1}) at 37 °C with agitation. *E. coli* strains DH5α, SM10, CC118λ*pir* and BL21(DE3) were used for cloning, conjugation and protein expression steps. *E. coli* cells were grown in TSB, LB, Terrific Broth or M9 minimal media (with indicated supplements), supplemented with antibiotics as appropriate (streptomycin 50 μg ml^{-1}, ampicillin 100 μg ml^{-1}, kanamycin 50 μg ml^{-1}) at 37 °C with agitation. *A. tumefaciens* C58 was grown in LB or M9 minimal media (with indicated supplements), supplemented with antibiotics as appropriate (gentamicin 50 μg ml^{-1}, spectinomycin 100 μg ml^{-1}) at 30 °C with agitation.

DNA manipulation. DNA isolation was performed using the PureLink Genomic DNA mini kit (Life Technologies) except for TraDIS library genomic DNA isolation (below). Isolation of plasmid DNA was carried out using the QIAprep spin miniprep kit (Qiagen). Primers (Sigma) used are shown in Supplementary Table 3. DNA fragments were amplified with either KOD Hot Start DNA Polymerase (Novagen) or standard Taq polymerase (NEB) as described by the manufacturer, with the inclusion of betaine (Sigma) or dimethylsulfoxide (Sigma). Restriction endonucleases (Roche) were used according to the manufacturer's specifications. DNA sequencing was performed by GATC Biotech.

TraDIS library generation. A highly saturated transposon mutant library was generated in *P. aeruginosa* PAKΔ*retS* or PAKΔ*retS*ΔH1 strains by large-scale conjugation with an *E. coli* SM10 [pBT20] donor which allowed for random insertion of a mariner transposon throughout the genome and conferred gentamicin resistance in the recipient PAK strain. The *E. coli* donor strain was grown in LB medium supplemented with gentamicin (15 μg ml^{-1}) overnight at 37 °C and the recipient PAK strain was grown overnight at 37 °C in LB medium. Equivalent amounts of both strains were spread uniformly on separate LB agar plates and incubated overnight at 37 °C for *E. coli* and at 43 °C under humid conditions for the PAK recipient. The next day, one *E. coli* donor plate was harvested and combined by extensive physical mixing on a fresh LB agar plate with one plate of harvested recipient PAK strain. Conjugation between the two strains was achieved by incubation of the high-density mixture of both strains at 37 °C for 2 h under humid conditions. The conjugation mix was then harvested, pelleted by centrifugation (10,000*g*, 10 min, 4 °C) and resuspended in LB medium. The resuspended cells were recovered onto large square (225 mm) Vogel-Bonner media (VBM) (8 mM $MgSO_4{\cdot}7H_2O$, 9.6 mM citric acid (anhydrous), 1.7 mM K_2HPO_4, 22.7 mM $NaNH_3PO_4{\cdot}4H_2O$, pH 7) agar plates supplemented with gentamicin (60 μg ml^{-1}) and incubated for 16 h at 37 °C. The numbers of mutants obtained were estimated by counting a representative number of colonies across multiple plates. Mutants for each library background on plates were recovered as two separate pools (T6SS active and T6SS inactive), resuspended in LB medium, pelleted by centrifugation (10,000*g*, 10 min, 4 °C), then resuspended in LB medium plus glycerol (15% v/v) and stored at −80 °C. The protocol was repeated on a large scale until ~2 million mutants were obtained in each library background. For the TraDIS assay, glycerol stocks of harvested PAKΔ*retS* or PAKΔ*retS*ΔH1 TraDIS libraries were combined at normalized cell density for each separate replicate (two final pools in total), spread onto large square (225 mm) VBM agar plates supplemented with gentamicin (60 μg ml^{-1}) and incubated for 16 h at 37 °C to facilitate T6SS delivery of toxins and subsequent killing/self-intoxication of mutants lacking immunity genes for the cognate toxin. Cells were then harvested into 5 ml of LB medium and pelleted by centrifugation (10,000*g*, 15 min, 4 °C). Cell pellets were resuspended in 1.4 ml of LB medium and 1 ml was retained for subsequent genomic DNA extraction ('TraDIS library genomic DNA extractions' below).

TraDIS library assay. Glycerol stocks of harvested PAKΔ*retS* or PAKΔ*retS*ΔH1 TraDIS libraries were combined at normalized cell density for each separate replicate and spread onto large square (225 mm) VBM agar plates supplemented with gentamicin (60 μg ml^{-1}) and incubated for 16 h at 37 °C. Cells were then harvested into 5 ml of LB medium and pelleted by centrifugation (10,000*g*, 15 min, 4 °C). Cell pellets were resuspended in 1.4 ml of LB medium and 1 ml was taken for subsequent genomic DNA extraction (below).

TraDIS library genomic DNA extractions. Genomic DNA from the harvested pooled library pellets either before or after undergoing the 'TraDIS library assay' (above) was resuspended in 1.2 ml of lysis solution (10 mM Tris–HCl, 400 mM NaCl and 2 mM Na_2EDTA, supplemented with Proteinase K in storage buffer (50 mM Tris–HCl, 50% v/v glycerol, 100 mM NaCl, 0.1 mM EDTA, 10 mM $CaCl_2$, 0.1% v/v Triton X-100 and 1 mM dithiothreitol) to a concentration of 166 μg ml^{-1}. Cell lysis was achieved by incubation at 65 °C for 1 h, with occasional vortexing. The samples were then cooled to room temperature and RNA removed by addition of RNase A (5 μg ml^{-1}) and incubation at 37 °C for 80 min. Samples were then placed on ice for 5 min. Each lysate was then split into two Eppendorf tubes at ~600 μl per tube, and 500 μl of NaCl (5 M) was added to each tube. Cell debris were removed by centrifugation (10,000*g*, 10 min, 4 °C) and 500 μl from each tube was added to 2 volumes of isopropanol to precipitate the DNA. DNA was then collected by centrifugation (10,000*g*, 10 min, 4 °C) and DNA pellets were washed twice in 70% (v/v) ethanol. The fully dried DNA pellet was finally resuspended in Tris–EDTA buffer.

PAK reference genome. The PAK genome under the NCBI number accession number LR657304, also listed in the European Nucleotide Archive under accession number ERS195106, was used. See details in Cain et al.[48]. PAK loci in Table 1, Extended Data Fig. 9 and throughout the text are the corresponding loci names from this genome.

Generation of TraDIS sequencing libraries, sequencing and downstream analysis. TraDIS sequencing was performed using the method described previously[23], with some minor modifications for this study, as described below. Also see Extended Data Fig. 10 and Supplementary Table 1.

Polymerase chain reaction primers were designed for library construction and used for both the PAK libraries (5′: AATGATACGGCGACCACCGAGATCTACACACAGGAAACAGGACTCTAGAGGATCACC and 3′: AATGATACGGCGACCACCGAGATCTACACCTTCTGTATGGAACGGGATGCG) and the sequencing TraDIS primers (5′: CAGCTTTCTTGTACACTAGAGACCGGGGACTTATCAG and 3′:AAGCCTGCTTTCTAGAGACCGGGGACTTATCAG). During library production, a postligation double digest with restriction enzymes AgeI and SgrAI was performed according to the manufacturer's instructions (New England Biolabs) to prevent amplification of plasmid background. T6SS TraDIS sequencing was performed on a HiSeq2500 Illumina platform on the RAPID 50 bp SE read setting. Reads were mapped onto the PAK genome (accession number: ERS195106), and comparisons were performed using the TraDIS Toolkit informatics package[23]. Ten per cent of the 3′-end of each gene was discounted, and a ten read minimum cut-off was included in the analysis. On average, there was a unique transposon insertion site every 53 bp over the whole genome for each of the T6SS active and T6SS inactive backgrounds and therefore the genome was highly saturated in each library. The distribution of transposon insertions across the genome based on the normalized transposon insertions in a H1-T6SS inactive library background, compared with the H1-T6SS active library background, is shown in Extended Data Fig. 10. The resulting sequences of the T6SS TraDIS assays are available from the European Nucleotide Archive under study accession number PRJEB1597.

To pinpoint genes involved in protection of T6SS-mediated killing, EdgeR[49] was used to identify significant differences in the read counts of genes in strains with (PAKΔ*retS*) and without (PAKΔ*retS*Δ*H1*) an active H1-T6SS. Trimmed mean of M values normalization was used to account for differences between the libraries, and tagwise dispersion was estimated. Only genes exhibiting more than five reads in both replicates of the conditions or control sets were examined for differences in the prevalence of mutants. Genes with zero read counts in the other condition were offset using the prior count function in EdgeR[49] so that fold changes could be estimated. *P* values were corrected for multiple testing using the Benjamini–Hochberg method, and genes with a corrected *P* value (*Q* value) of <0.05 (5% false discovery rate) and an absolute $\log_2$(fold change) ($\log_2$FC) of >2 were considered significant (see Tab 2 in Supplementary Table 1). The result was a list of 49 genes having statistically significant decreased insertions in the T6SS active library PAKΔ*retS* compared with normalized values in the PAKΔ*retS*Δ*HI* library. These genes were interrogated as potential immunities, based first on gene size (the known H1-T6SS associated immunity genes (*tsi1–6*) at the time of analysis are all less than 600 bp, thus this was used as a guide to shorten the list to 29 genes; see Tab 3 in Supplementary Table 1) and also on whether a protein upstream of these genes appeared to have a predicted enzymatic or putative toxin function.

Bacterial growth assays. Growth assays were performed as follows. For Fig. 1a, overnight cultures of PAKΔ*retS*Δ*tsei8* were diluted to OD_{600} = 0.1 in M9 minimal

media supplemented with $MgSO_4$ (2 mM), $CaCl_2$ (0.1 mM), glucose (0.4% w/v) and $FeSO_4{\cdot}7H_2O$ (0.01 mM), and grown with shaking at 37 °C. Expression of Tse8 was induced with isopropyl-β-D-thiogalactoside (IPTG) (1 mM) at 4 h. For Fig. 1d, PAKΔ*retS*Δ*tsei8* cells carrying both pJN105 and pMMB67HE plasmids (+/− Tsi8/Tse8) were grown in MOPS minimal media (MOPS (40 mM, pH 7.5), tricine (4 mM, pH 7.5), NH_4Cl (9.52 mM), $CaCl_2$ (0.5 µM), $MgCl_2{\cdot}7H_2O$ (0.52 mM), NaCl (50 mM), $FeSO_4{\cdot}7H_2O$ 20 mM (0.01 mM), K_2HPO_4 (1.32 mM)) supplemented with 1× micronutrient mix (100×: ammonium molybdate tetrahydrate (3 µM), boric acid (400 µM), cobalt chloride (30 µM), cupric sulfate (10 µM), manganese chloride (80 µM), zinc sulfate (10 µM) and nickel chloride hexahydrate (0.1% w/v)), glucose (0.4% w/v), and L-glutamine (0.05% w/v) with shaking at 37 °C (without antibiotics). Expression of Tse8 was induced with IPTG (1 mM) and Tsi8 with arabinose (0.2% w/v) at 5 h. For Fig. 3a, overnight cultures of *A. tumefaciens* with pTrc200/pJN105 plasmids (+/− Tse8/Tsi8) were diluted to OD_{600} = 0.1 in MOPS media without antibiotics as above and grown with shaking at 30 °C. Expression of Tse8 was induced with IPTG (1 mM) and Tsi8 with arabinose (0.2% w/v) at 8 h. For Fig. 3b, overnight cultures of *E. coli* were diluted to OD_{600} = 0.1 in M9 minimal media (supplemented with 2 mM $MgSO_4$, 0.1 mM $CaCl_2$, 0.01 mM $FeSO_4{\cdot}7H_2O$ and 0.4% w/v glucose) and grown with shaking at 37 °C. Tse8 expression was induced with IPTG (1 mM) after 2 h. For Fig. 4b, overnight cultures of the indicated *P. aeruginosa* strain were diluted to OD_{600} = 0.1 in LB medium (without antibiotics) and grown with shaking at 37 °C. Expression of Tse8 was induced with IPTG (0.25 mM) and Tsi8 or AsnS with arabinose (0.2% w/v) at 0 h.

T6SS competition assays. T6SS competition assays were performed as described previously[50] with modifications as indicated. Briefly, overnight cultures of donor and recipient bacteria alone or in a 1:1 ratio were combined and spot plated on LB agar plates for 5 h at 37 °C and recovered in serial dilution on LB agar plates supplemented with 5-bromo-4-chloro-3-indolyl-β-D-galactopyranoside (Xgal; 100 µg ml^{-1}) to differentiate recipient (PAKΔ*retS*Δ*tsei8*::*lacZ* seen as blue) from donor (white). For recovery of competition assays between donor and recipient PAKΔ*retS*Δ*tsei8* [pBBR1-MCS5] and [pBBR1:*tsei8*], the competition assay was plated onto LB agar plates with gentamicin (50 µg ml^{-1}) to differentiate donor from recipient (Gm^R). For recovery of competition assays between donor and recipient PAKΔ*retS*Δ*tsei8* [pBBR1-MCS4] and [pBBR4:*tse8*], the competition assay was plated onto LB agar plates with carbenicillin (50 µg ml^{-1}) to differentiate donor from recipient ($Carb^R$). In other cases, expression of Tsi8 or AsnS in the recipient strains was induced in the overnight cultures by addition of arabinose (0.2% w/v). These overnight cultures of donor and induced recipient alone or in a 1:1 ratio were combined and spot plated onto LB agar supplemented with arabinose (1% w/v) for induction of Tsi8-V5 or AsnS-His for 5 h, with the competition assay finally being recovered on LB agar plates supplemented with gentamycin (50 µg ml^{-1}) and arabinose (1% w/v).

BTH and β-galactosidase assays. Protein–protein interactions were analysed using the BTH system as described previously[51]. Briefly, the DNA regions encoding the protein of interest was amplified by polymerase chain reaction and then cloned into plasmids pKT25 and pUT18C, which each encode for complementary fragments of the adenylate cyclase enzyme, as previously described[51] resulting in N-terminal fusions of T25/T18 from the adenylate cyclase to the protein of interest. Recombinant pKT25 and pUT18c plasmids were used simultaneously to transform the *E. coli* DHM1 strain, which lacks adenylate cyclase, and transformants were spotted onto Xgal (40 µg ml^{-1}) LB agar plates supplemented with IPTG (1 mM), kanamycin (50 µg ml^{-1}) and ampicillin (100 µg ml^{-1}). Positive interactants were identified after incubation at 30 °C for 48 h. The positive controls used in the study were pUT18C or pKT25 derivatives encoding the leucine zipper from GCN4, which forms a dimer under the assay conditions. The strength of the interactions in the BTH assays was quantified from the β-galactosidase activity of cotransformants scraped from Xgal plates and measured as described previously; activity was calculated in Miller units[51].

Western blot analysis. SDS–PAGE and western blotting were performed as described previously[11]. Proteins were resolved in 8%, 10%, 12% or 15% gels using the Mini-PROTEAN system (Bio-Rad) and transferred to a nitrocellulose membrane (GE Healthcare) by electrophoresis. Membranes were blocked in 5% (w/v) milk (Sigma) before incubation with primary antibodies (anti-His at 1:1,000 dilution and anti-V5 or anti-HA at 1:5,000 dilution). Membranes were washed with TBST (0.14 M NaCl, 0.03 M KCl and 0.01 M phosphate buffer plus Tween 20 (0.05% v/v)) before incubation with horseradish peroxidase (HRP)-conjugated secondary antibodies (Sigma; anti-mouse at 1:5,000 dilution). The resolved proteins on the membrane blots were detected using the Novex ECL HRP Chemiluminescent substrate (Invitrogen) or the Luminata Forte Western HRP substrate (Millipore) using a Las3000 Fuji Imager. For Fig. 3c, samples were taken after 8 h of growth and expression of Tse8 was assessed by western blot as above; detection of Tse8 was performed using anti-HA antibody (1:5,000 dilution).

Dot blotting. For Tse8 interactions with VgrG1a, VgrG1b and VgrG1c, purified untagged Tse8 was spotted onto a nitrocellulose membrane (3 mg ml^{-1}) and dried at room temperature. Membranes were blocked with TBST with 5% (w/v) milk or 2.5% (w/v) bovine serum albumin for 7 h at room temperature. *E. coli* overexpressing VgrG1a–V5, VgrG1b–V5, VgrG1c–V5 or CcmE–His (equivalent 150 OD_{600} units) were pelleted and then resuspended in 10 ml of 100 mM NaCl, 20 mM Tris, 10% (w/v) glycerol, 2% (w/v) milk powder and 0.1% (v/v) Tween 20 (Tween 20 was added after sonication) (pH 7.6) and sonicated. Ten millilitres of the crude lysates were applied directly to the membranes and incubated overnight at room temperature. The membranes were immunoblotted with anti-V5 (1:5,000 Invitrogen) or anti-His (1:1,000 Sigma) overnight at 4 °C and anti-mouse secondary (1:5,000). Quantification of dot blots was performed using the Gel Analyzer plugin in ImageJ[52]. Levels were normalized to the control signal based on three independent experiments.

Pull-down experiments. *E. coli* BL21(DE3) strains expressing simultaneously GatA–V5, GatB–His and GatC–HA or GatB–His and GatC–HA were grown in LB medium at 37 °C to an OD_{600} of 0.8 and expression was subsequently induced using 1 mM IPTG (Sigma) for 16 h at 18 °C. *E. coli* BL21(DE3) cells expressing Tse8–HA-Strep were grown in Terrific Broth at 37 °C to an OD_{600} of 0.8 and expression was subsequently induced using 1 mM IPTG (Sigma) for 16 h at 30 °C. The same expression strategy used for Tse8–HA-Strep was also used for *E. coli* BL21(DE3) strains expressing Tsi8–His or CcmE–His except that TSB medium was used. Cell pellets resulting during expression of GatCAB, GatBC, Tsi8 or CcmE were resuspended in buffer A (50 mM Tris–HCl, 150 mM NaCl, 20 mM imidazole, pH 7.5) and lysed by sonication after the addition of protease inhibitors (Roche). Cell debris were eliminated by centrifugation (48,000*g*, 30 min, 4 °C). Proteins were purified by immobilized metal affinity chromatography using nickel–Sepharose resin (GE Healthcare) equilibrated in buffer A. Proteins were then eluted off the resin with buffer A containing 200 mM instead of 20 mM imidazole. Cell pellets resulting during expression of Tse8 were resuspended in 50 mM Tris–HCl, 150 mM NaCl (pH 7.5) and lysed by sonication after the addition of protease inhibitors (Roche). Tse8–HA-Strep was purified using Strep-Tactin Sepharose (IBA Lifesciences), according to the manufacturer's specifications.

For pull-down experiments using pure proteins, the above purified protein solutions and His-Tag Isolation & Pull Down Dynabeads (Thermo Fisher Scientific) were used. Briefly, the appropriate protein mixtures were generated by mixing 40 µM of the bait protein with equimolar amounts of Tse8–HA-Strep (Tsi8 bait) or 15-fold molar excess of Tse8–HA-Strep (GatCAB bait); a condition containing solely the same amount of Tse8–HA-Strep was also tested as a negative binding control. Mixtures were added to a 25-µl bed of Dynabeads and incubated at 25 °C with agitation for 1 h, before the beads were washed eight times with 800 µl of wash buffer (50 mM Tris pH 7.5, 150 mM NaCl, 0.01% Tween 20) and resuspended in elution buffer (50 mM Tris pH 7.5, 150 mM NaCl, 0.01% Tween 20, 200 mM imidazole).

For pull-down experiments using purified GatCB and cell lysates containing GatA–V5 and Tse8–HA-StrepII, 150 OD_{600} units of cells expressing GatA–V5 and Tse8–HA-StrepII were resuspended in binding buffer (20 mM Tris pH 7.5, 100 mM NaCl, 10% v/v glycerol and 3% w/v bovine serum albumin) and lysed by sonication. Pull-downs were performed by adding a total volume of 6 ml of cell lysate (3 ml of GatA–V5 lysate mixed with 3 ml of binding buffer or 3 ml of GatA–V5 lysate mixed with 3 ml of Tse8–HA-StrepII lysate) to a 25-µl bed of His-Tag Isolation & Pull Down Dynabeads (Thermo Fisher Scientific) loaded with 40 µg of purified GatCB. Mixtures were incubated at 25 °C with agitation for 1 h before the beads were washed 8× with 800 µl of wash buffer (50 mM Tris pH 7.5, 150 mM NaCl, 0.01% Tween 20) and resuspended in elution buffer (50 mM Tris pH 7.5, 150 mM NaCl, 0.01% Tween 20, 200 mM imidazole).

For all experiments, eluted samples were denatured in 4× Laemmli buffer and subjected to western blotting as described above. Anti-V5 (1:5,000 Invitrogen), anti-HA (1:5,000 Biolegend) or anti-His (1:1,000 Sigma) primary antibodies were used along with an anti-mouse secondary antibodies (1:5,000 Sigma). For detection of StrepII tags a Strep-Tactin HRP conjugate was used (1:3,000 IBA Lifesciences). Quantification of western blot bands was performed using the Gel Analyzer plugin in ImageJ[52].

Whole-cell glutaminase assays. The whole-cell glutaminase activity was measured as described previously[53] with some modifications as follows. *E. coli* B834 cells containing empty vector, *gatA* or *tse8* in pET41a were grown to OD_{600} ~0.6 when expression was induced by addition of IPTG (0.5 mM) and grown at 18 °C for 16 h. Cells pellets equivalent to 45 OD_{600} units were washed in sodium acetate solution (100 mM sodium acetate, pH 6, 20 mM L-glutamine) and resuspended in a final volume of 600 µl of sodium acetate solution, and incubated at 37 °C for 30 min. Some 20 µl of cells were retained and serially diluted to quantify the number of c.f.u. present. The remaining cell volume was then lysed by heating at 99 °C for 3 min. Once cooled to room temperature, 100 µl of cell lysate was added to 2 ml of glutamate dehydrogenase solution (10 mM sodium acetate, 4 mM NAD^+, 400 mM hydroxylamine HCl, 30 U of glutamate dehydrogenase (GDH) enzyme (Sigma) in 100 mM potassium phosphate buffer, pH 7.2) and incubated at 60 °C for 60 min. A 150-µl aliquot of the reaction was added to a 96-well clear plate and the relative accumulation of NADPH was calculated using the measured absorbance at 340 nm.

Expression and purification of Tse8 used for activity measurements. The pET41a::GST-TEV-Tse8 vector coding for *P. aeruginosa* Tse8 was obtained by

FastCloning[54] using pET41a:GST-Tse8 (Supplementary Table2) as the template. This construct was subcloned using the forward primer 5′-AACCTGTATTTTCA GGGCGGATCCATCGAGGTCACCGAGGTTTCCATCG-3′ and reverse primer 5′-CCTGAAAATACAGGTTTTCGGTACCCAGATCTGGGCTGTCCATGTGCT GG-3′ to exchange the *Human Rhinovirus* (HRV) 3C cleavage site (LEVLFQ/GP) with a TEV protease cleavage site (ENLYFQ/G). The resulting construct includes: (1) a 651-nucleotide sequence encoding a N-terminal glutathione *S*-transferase (GST) tag; (2) an 18-nucleotide sequence encoding a 6× histidine tag; and (3) a 45-nucleotide sequence encoding a S15 tag and a 21-nucleotide sequence encoding the optimal tobacco etch virus (TEV) protease cleavage site Glu–Asn–Leu–Tyr–Phe–Gln–Gly (Extended Data Fig. 5). For protein expression, *E. coli* BL21(DE3) cells were transformed with the pET41a::GST-TEV-Tse8 plasmid and grown in 2× Yeast Extract Tryptone medium (supplemented with 50 μg ml^{-1} kanamycin) at 37 °C. When the culture reached an OD_{600} value of 0.7, Tse8 expression was induced by adding 1 mM IPTG and the temperature was dropped to 18 °C. After 18 h, cells were harvested and frozen for later use.

For protein purification, each 1-L pellet was resuspended in 50 ml of 50 mM Tris–HCl pH 8, 500 mM NaCl, 20 mM imidazole, 0.5 mM EDTA and 2 μl of benzonase endonuclease (without addition of protease inhibitors). Cells were then disrupted by sonication and the suspension was centrifuged for 40 min at 56,000*g*. The supernatant was filtered with a 0.2-μm syringe filter and subjected to immobilized metal affinity chromatography using a 1 ml HisTrap HP column (GE Healthcare), on a fast protein liquid chromatography system (ÄKTA FPLC; GE Healthcare) equilibrated with 5 ml of 50 mM Tris–HCl pH 8, 500 mM NaCl and 20 mM imidazole (buffer A). The column was washed with buffer A at 1 ml min^{-1} until no absorbance at 280 nm was detected. Elution was performed with a linear gradient between 0% and 50% of 50 mM Tris–HCl pH 8, 500 mM NaCl and 500 mM imidazole in 30 ml and at 1 ml min^{-1}. Fractions containing GST–TEV–Tse8 fusion protein were pooled and protein concentration was measured. The cleavage of the GST–His–S15 tag was performed with TEV protease (1 mg per 10 mg of protein) overnight at 18 °C in buffer 50 mM Tris–HCl pH 7.5, 2 mM dithiothreitol, at a protein concentration between 0.3 and 0.5 mg ml^{-1}. The cleaved Tse8, non-cleaved Tse8 and TEV protease were collected, filtered and applied onto a HisTrap HP column (5 ml; GE Healthcare) equilibrated with 25 ml of 50 mM Tris–HCl pH 7.5. The cleaved Tse8 was eluted in the flow-through and applied onto a Mono Q column of 5 ml (GE Healthcare) equilibrated with 25 ml of 50 mM Tris–HCl pH 7.5. The protein was eluted in a single step using 500 mM NaCl in 50 mM Tris–HCl pH 7.5. The Tse8 protein was dialysed with 20 mM sodium phosphate buffer pH 7.6 and concentrated using Centricon centrifugal filter units of 30 kDa molecular mass cut-off (Millipore) to a final concentration of 5 mg ml^{-1} for enzymatic assays. The purity of the protein was verified by SDS–PAGE (Extended Data Fig. 5) and protein integrity was evaluated following desalting with stage-tip C_4 microcolumns (Zip-tip, Millipore) by electrospray ionization mass spectrometry (ESI-MS). The sampling cone energy was set at 35 V. The *m*/*z* data were then deconvoluted into MS data using MaxEnt software (MaxEnt Solutions Ltd) with a resolution of the output mass of 0.5 Da/channel and Uniform Gaussian Damage Model at the half height of 0.5 Da. The analysis indicates that 90% of the protein sample corresponds to the expected Tse8 molecular mass (60,564 Da; Extended Data Fig. 5).

Tse8 substrate activity assays. Putative Tse8 substrates were selected based on the predicted GatA and Pam homology. Thus, the capacity of Tse8 to hydrolyse carbon–nitrogen bonds was analysed by MS using as putative substrates the free amino acid glutamine and the C-terminally amidated peptide epinecidin-1 (sequence: GFIFHIIKGLFHAGKMIHGLV-NH_2; Bachem AG). Glutamine (10 mM) was incubated with 2 μM of freshly purified Tse8. Reactions were carried out in two different buffers to test the possible effect of pH; one set of reactions was carried out in 10 mM sodium phosphate buffer (pH 7.6) and the other in 20 mM Tris–HCl buffer (pH 8.3). For epinecidin-1, 5 μM of freshly purified Tse8 or the positive control protein Pam (purified as described previously[55]), were incubated with 50 μM of putative substrate in 10 mM sodium phosphate buffer (pH 7.2); control reactions, lacking Tse8 or Pam, were also tested. Reactions were incubated overnight at 30 °C, followed by MS analysis. For full details on the MS analysis see the relevant section below for use of epinecidin-1 or glutamine as a substrate.

Mass spectrometry analysis of Tse8/Pam enzymatic assays using epinecidin-1 as a substrate. Samples were desalted and peptides were isolated using stage-tip C_{18} microcolumns (Zip-tip, Millipore) and further resuspended in 0.1% formic acid before MS analysis. Peptide separation was performed on a nanoACQUITY ultrapure liquid chromatograohy (UPLC) system (Waters) online connected to an LTQ Orbitrap XL mass spectrometer (Thermo Electron). An aliquot of each sample was loaded onto a Symmetry 300 C_{18} UPLC Trap column (180 μm × 20 mm, 5 μm; Waters). The precolumn was connected to a BEH130 C_{18} column (75 μm × 200 mm, 1.7 μm; Waters), and equilibrated in 3% acetonitrile and 0.1% formic acid. Peptides were eluted directly into an LTQ Orbitrap XL mass spectrometer (Thermo Finnigan) through a nanoelectrospray capillary source (Proxeon Biosystems) at 300 nl min^{-1} and using a 120 min linear gradient of 3–50% acetonitrile. The mass spectrometer automatically switched between MS and tandem MS acquisition in DDA mode. Full MS scan survey spectra (*m*/*z* 400–2,000) were acquired in the orbitrap with mass resolution of 30,000 at *m*/*z* 400. After each survey scan, the six most intense ions above 1,000 counts were sequentially subjected to collision-induced dissociation in the linear ion trap. Precursors with charge states of 2 and 3 were specifically selected for collision-induced dissociation. Peptides were excluded from further analysis during 60 s using the dynamic exclusion feature. RAW files were searched with the Mascot search engine (www.matrixscience.com) through Proteome Discoverer v.1.4 (Thermo) against a FASTA database containing the protein and peptide sequences of interest, together with a *Pichia pastoris* database from Uniprot/Swissprot as a background. Search parameters were: 10 ppm peptide mass tolerance, 0.5 Da fragment mass tolerance, carbamydomethylation of cysteines as fixed modification, and oxidation of methionine, amidation and deamidation of protein C terminus as variable modifications. Only highly reliable hits (P<0.01) were considered.

Mass spectrometry analysis of Tse8 enzymatic assay using glutamine as substrate. Overnight incubations were quenched by addition of 150 μl of 20% acetonitrile (MeCN). Controls for the experiment were prepared by first adding MeCN to the reaction blank and subsequently adding enzyme. To determine liquid chromatography–mass spectrometry performance, 100 μM stock solutions of glutamine substrate in 2:3 water/MeCN were injected before the experimental samples. Quenched incubations and controls were shaken in the tubes for 30 min at 4 °C and 1,000*g*. Samples were then centrifuged for 30 min at 4 °C and 25,000*g*. The resulting solutions were immediately injected into the liquid chromatography–mass spectrometer. Samples were measured with a UPLC system (Acquity, Waters Inc.) coupled to a time-of-flight mass spectrometer (SYNAPT G2, Waters Inc.). A 2.1 × 100 mm, 1.7 μm BEH amide column (Waters Inc.), thermostated at 40 °C, was used to separate the analytes before entering the mass spectrometer. Mobile phase solvent A (aqueous phase) consisted of 99.5% water, 0.5% formic acid and 20 mM ammonium formate, whereas solvent B (organic phase) consisted of 29.5% water, 70% MeCN, 0.5% formic acid and 1 mM ammonium formate. To obtain good separation of the analytes, the following gradient was used: from 5% A to 50% A in 2.4 min in curved gradient (no. 8, as defined by Waters), from 50% A to 99.9% A in 0.2 min, constant at 99.9% A for 1.2 min, and finally back to 5% A in 0.2 min. The flow rate was 0.250 ml min^{-1} and the injection volume was 2 μl. The mass spectrometer was operated in positive (ESI+) and negative (ESI−) electrospray ionization in full-scan mode. The cone voltage was 25 V and the capillary voltage was 250 V for ESI+ and 500 V for ESI−. The source temperature was set to 120 °C and the capillary temperature to 450 °C. The flow of the cone and desolvation gas (both nitrogen) were set to 5 and 600 L h^{-1}, respectively. A 2 ng ml^{-1} leucine–enkephalin solution in water/acetonitrile/formic acid (49.9:50:0.1% v/v/v) was infused at 10 μl min^{-1} and used for a lock mass, which was measured every 36 s for 0.5 s. Spectral peaks were corrected automatically for deviations in the lock mass.

Bioinformatics analysis of prokaryotic organisms encoding AsnS and GlnS. *E. coli* AsnS and GlnS protein sequences were interrogated against the National Center for Biotechnology Information (NCBI) collection of non-redundant protein sequences of bacteria and archaea (non-redundant Microbial proteins, update: 2017/11/29) using the pBLAST search engine. The search was further restricted for non-redundant RefSeq proteins, with a 20,000-hit limit, the BLOSUM62 matrix scoring function and an Expect threshold value (*E*-value) of 1×10^{-5}. Hits were selected if sequence identity was above 50% with respect to the query sequences and those associated with bacterial species *A. tumefaciens, E. coli* and *P. aeruginosa* were extracted (Supplementary Table 4).

Bioinformatics analysis of prokaryotic organisms predicted to encode the amidotransferase GatCAB complex. A non-exhaustive search for organisms encoding GatCAB was carried out using the NCBI database. *P. aeruginosa* GatA and GatB protein sequences were interrogated against the NCBI collection of non-redundant protein sequences of bacteria and archaea (non-redundant Microbial proteins, update: 2017/11/29) using the pBLAST search engine. The search was further restricted for non-redundant RefSeq proteins, with a 20,000-hit limit, BLOSUM62 matrix scoring function and an *E*-value of 1×10^{-5}. Hits were selected if annotated as Asp-tRNA(Asn)/Glu-tRNA(Gln) amidotransferase subunits, and the results for *A. tumefaciens, E. coli* and *P. aeruginosa* were extracted (Supplementary Table 4).

Statistical analyses. Statistical analyses were performed using GraphPad Prism v.9 and are detailed in the figure legends.

Reporting Summary. Further information on the research design is available in the Nature Research Reporting Summary linked to this article.

Data availability

PAK genome NCBI number is LR657304, and in the ENA (European Nucleotide Archive) the accession code is ERS195106. The resulting sequences of the T6SS TraDIS assays are available from the ENA under study accession number ERS577921. Source data are provided with this paper.

Received: 14 June 2018; Accepted: 15 July 2021
Published online: 19 August 2021

References

1. Sibley, C. D. et al. A polymicrobial perspective of pulmonary infections exposes an enigmatic pathogen in cystic fibrosis patients. *Proc. Natl Acad. Sci. USA* **105**, 15070–15075 (2008).
2. Peters, B. M., Jabra-Rizk, M. A., O'May, G. A., Costerton, J. W. & Shirtliff, M. E. Polymicrobial interactions: impact on pathogenesis and human disease. *Clin. Microbiol. Rev.* **25**, 193–213 (2012).
3. Bingle, L. E., Bailey, C. M. & Pallen, M. J. Type VI secretion: a beginner's guide. *Curr. Opin. Microbiol.* **11**, 3–8 (2008).
4. Pukatzki, S., McAuley, S. B. & Miyata, S. T. The type VI secretion system: translocation of effectors and effector-domains. *Curr. Opin. Microbiol.* **12**, 11–17 (2009).
5. Cianfanelli, F. R., Monlezun, L. & Coulthurst, S. J. Aim, load, fire: the type VI secretion system, a bacterial nanoweapon. *Trends Microbiol.* **24**, 51–62 (2016).
6. Filloux, A. Microbiology: a weapon for bacterial warfare. *Nature* **500**, 284–285 (2013).
7. Nazarov, S. et al. Cryo-EM reconstruction of Type VI secretion system baseplate and sheath distal end. *EMBO J.* **37**, e97103 (2018).
8. Shneider, M. M. et al. PAAR-repeat proteins sharpen and diversify the type VI secretion system spike. *Nature* **500**, 350–353 (2013).
9. Wang, J. et al. Cryo-EM structure of the extended type VI secretion system sheath–tube complex. *Nat. Microbiol* **2**, 1507–1512 (2017).
10. Kudryashev, M. et al. Structure of the type VI secretion system contractile sheath. *Cell* **160**, 952–962 (2015).
11. Hachani, A., Allsopp, L. P., Oduko, Y. & Filloux, A. The VgrG proteins are "a la carte" delivery systems for bacterial type VI effectors. *J. Biol. Chem.* **289**, 17872–17884 (2014).
12. Ma, J. et al. The Hcp proteins fused with diverse extended-toxin domains represent a novel pattern of antibacterial effectors in type VI secretion systems. *Virulence* **8**, 1189–1202 (2017).
13. Silverman, J. M. et al. Haemolysin coregulated protein is an exported receptor and chaperone of type VI secretion substrates. *Mol. Cell* **51**, 584–593 (2013).
14. Whitney, J. C. et al. Genetically distinct pathways guide effector export through the type VI secretion system. *Mol. Microbiol.* **92**, 529–542 (2014).
15. Russell, A. B. et al. A widespread bacterial type VI secretion effector superfamily identified using a heuristic approach. *Cell Host Microbe* **11**, 538–549 (2012).
16. Russell, A. B., Peterson, S. B. & Mougous, J. D. Type VI secretion system effectors: poisons with a purpose. *Nat. Rev. Microbiol.* **12**, 137–148 (2014).
17. Hood, R. D. et al. A type VI secretion system of *Pseudomonas aeruginosa* targets a toxin to bacteria. *Cell Host Microbe* **7**, 25–37 (2010).
18. Allsopp, L. P. et al. RsmA and AmrZ orchestrate the assembly of all three type VI secretion systems in *Pseudomonas aeruginosa*. *Proc. Natl Acad. Sci. USA* **114**, 7707–7712 (2017).
19. Cain, A. K. et al. A decade of advances in transposon-insertion sequencing. *Nat. Rev. Genet.* **21**, 526–540 (2020).
20. Dong, T. G., Ho, B. T., Yoder-Himes, D. R. & Mekalanos, J. J. Identification of T6SS-dependent effector and immunity proteins by Tn-seq in *Vibrio cholerae*. *Proc. Natl Acad. Sci. USA* **110**, 2623–2628 (2013).
21. Ibba, M., Becker, H. D., Stathopoulos, C., Tumbula, D. L. & Soll, D. The adaptor hypothesis revisited. *Trends Biochem. Sci.* **25**, 311–316 (2000).
22. Langridge, G. C. et al. Simultaneous assay of every *Salmonella typhi* gene using one million transposon mutants. *Genome Res.* **19**, 2308–2316 (2009).
23. Barquist, L. et al. The TraDIS toolkit: sequencing and analysis for dense transposon mutant libraries. *Bioinformatics* **32**, 1109–1111 (2016).
24. Pissaridou, P. et al. The *Pseudomonas aeruginosa* T6SS-VgrG1b spike is topped by a PAAR protein eliciting DNA damage to bacterial competitors. *Proc. Natl Acad. Sci. USA* **115**, 12519–12524 (2018).
25. Jiang, F., Waterfield, N. R., Yang, J., Yang, G. & Jin, Q. A *Pseudomonas aeruginosa* type VI secretion phospholipase D effector targets both prokaryotic and eukaryotic cells. *Cell Host Microbe* **15**, 600–610 (2014).
26. Whitney, J. C. et al. An interbacterial NAD(P)$^+$ glycohydrolase toxin requires elongation factor Tu for delivery to target cells. *Cell* **163**, 607–619 (2015).
27. Kelley, L. A., Mezulis, S., Yates, C. M., Wass, M. N. & Sternberg, M. J. The Phyre2 web portal for protein modeling, prediction and analysis. *Nat. Protoc.* **10**, 845–858 (2015).
28. Labahn, J., Neumann, S., Buldt, G., Kula, M. R. & Granzin, J. An alternative mechanism for amidase signature enzymes. *J. Mol. Biol.* **322**, 1053–1064 (2002).
29. Nakamura, A., Yao, M., Chimnaronk, S., Sakai, N. & Tanaka, I. Ammonia channel couples glutaminase with transamidase reactions in GatCAB. *Science* **312**, 1954–1958 (2006).
30. Suzuki, T. et al. Structure of the *Pseudomonas aeruginosa* transamidosome reveals unique aspects of bacterial tRNA-dependent asparagine biosynthesis. *Proc. Natl Acad. Sci. USA* **112**, 382–387 (2015).
31. Yasuhira, K. et al. X-ray crystallographic analysis of the 6-aminohexanoate cyclic dimer hydrolase: catalytic mechanism and evolution of an enzyme responsible for nylon-6 byproduct degradation. *J. Biol. Chem.* **285**, 1239–1248 (2010).
32. Shin, S. et al. Characterization of a novel Ser–*cis*Ser–Lys catalytic triad in comparison with the classical Ser–His–Asp triad. *J. Biol. Chem.* **278**, 24937–24943 (2003).
33. Balotra, S. et al. X-ray structure of the amidase domain of AtzF, the allophanate hydrolase from the cyanuric acid–mineralizing multienzyme complex. *Appl. Environ. Microbiol.* **81**, 470–480 (2015).
34. Lee, S. et al. Crystal structure analysis of a bacterial aryl acylamidase belonging to the amidase signature enzyme family. *Biochem. Biophys. Res. Commun.* **467**, 268–274 (2015).
35. Ruan, L. T., Zheng, R. C. & Zheng, Y. G. Mining and characterization of two amidase signature family amidases from *Brevibacterium epidermidis* ZJB-07021 by an efficient genome mining approach. *Protein Expr. Purif.* **126**, 16–25 (2016).
36. Valina, A. L., Mazumder-Shivakumar, D. & Bruice, T. C. Probing the Ser–Ser–Lys catalytic triad mechanism of peptide amidase: computational studies of the ground state, transition state, and intermediate. *Biochemistry* **43**, 15657–15672 (2004).
37. Wei, B. Q., Mikkelsen, T. S., McKinney, M. K., Lander, E. S. & Cravatt, B. F. A second fatty acid amide hydrolase with variable distribution among placental mammals. *J. Biol. Chem.* **281**, 36569–36578 (2006).
38. Shin, S. et al. Structure of malonamidase E2 reveals a novel Ser–*cis*Ser–Lys catalytic triad in a new serine hydrolase fold that is prevalent in nature. *EMBO J.* **21**, 2509–2516 (2002).
39. Patricelli, M. P. & Cravatt, B. F. Clarifying the catalytic roles of conserved residues in the amidase signature family. *J. Biol. Chem.* **275**, 19177–19184 (2000).
40. Akochy, P. M., Bernard, D., Roy, P. H. & Lapointe, J. Direct glutaminyl-tRNA biosynthesis and indirect asparaginyl-tRNA biosynthesis in *Pseudomonas aeruginosa* PAO1. *J. Bacteriol.* **186**, 767–776 (2004).
41. González-Magaña, A. et al. Structural insights into *Pseudomonas aeruginosa* type six secretion system exported effector 8. *J. Struct. Biol.* **212**, 107651 (2020).
42. Bernal, P., Allsopp, L. P., Filloux, A. & Llamas, M. A. The *Pseudomonas putida* T6SS is a plant warden against phytopathogens. *ISME J.* **11**, 972–987 (2017).
43. Filloux, A., Hachani, A. & Bleves, S. The bacterial type VI secretion machine: yet another player for protein transport across membranes. *Microbiology* **154**, 1570–1583 (2008).
44. Shalom, G., Shaw, J. G. & Thomas, M. S. *In vivo* expression technology identifies a type VI secretion system locus in *Burkholderia pseudomallei* that is induced upon invasion of macrophages. *Microbiology* **153**, 2689–2699 (2007).
45. Zhang, W. et al. Modulation of a thermoregulated type VI secretion system by AHL-dependent quorum sensing in *Yersinia pseudotuberculosis*. *Arch. Microbiol.* **193**, 351–363 (2011).
46. Kaniga, K., Delor, I. & Cornelis, G. R. A wide-host-range suicide vector for improving reverse genetics in gram-negative bacteria: inactivation of the *blaA* gene of *Yersinia enterocolitica*. *Gene* **109**, 137–141 (1991).
47. Hachani, A. et al. Type VI secretion system in *Pseudomonas aeruginosa*: secretion and multimerization of VgrG proteins. *J. Biol. Chem.* **286**, 12317–12327 (2011).
48. Cain, A. K. et al. Complete genome sequence of *Pseudomonas aeruginosa* reference strain PAK. *Microbiol. Resour. Announc.* **8**, e00865–19 (2019).
49. Robinson, M. D., McCarthy, D. J. & Smyth, G. K. edgeR: a Bioconductor package for differential expression analysis of digital gene expression data. *Bioinformatics* **26**, 139–140 (2010).
50. Hachani, A., Lossi, N. S. & Filloux, A. A visual assay to monitor T6SS-mediated bacterial competition. *J. Vis. Exp.* **73**, e50103 (2013).
51. Karimova, G., Pidoux, J., Ullmann, A. & Ladant, D. A bacterial two-hybrid system based on a reconstituted signal transduction pathway. *Proc. Natl Acad. Sci. USA* **95**, 5752–5756 (1998).
52. Schindelin, J. et al. Fiji: an open-source platform for biological-image analysis. *Nat. Methods* **9**, 676–682 (2012).
53. Sato, I. et al. *Cryptococcus nodaensis* sp nov, a yeast isolated from soil in Japan that produces a salt-tolerant and thermostable glutaminase. *J. Ind. Microbiol. Biotechnol.* **22**, 127–132 (1999).
54. Li, C. et al. FastCloning: a highly simplified, purification-free, sequence- and ligation-independent PCR cloning method. *BMC Biotechnol.* **11**, 92 (2011).
55. Wu, B. et al. Versatile peptide C-terminal functionalization via a computationally engineered peptide amidase. *ACS Catal.* **6**, 5405–5414 (2016).
56. Barquist, L., Boinett, C. J. & Cain, A. K. Approaches to querying bacterial genomes with transposon-insertion sequencing. *RNA Biol.* **10**, 1161–1169 (2013).

57. Edgar, R. C. MUSCLE: multiple sequence alignment with high accuracy and high throughput. *Nucleic Acids Res.* **32**, 1792–1797 (2004).
58. Robert, X. & Gouet, P. Deciphering key features in protein structures with the new ENDscript server. *Nucleic Acids Res.* **42**, W320–W324 (2014).

Acknowledgements

L.M.N. was supported by Medical Research Council (MRC) Grant MR/N023250/1 and a Marie Curie Fellowship (PIIF-GA-2013-625318). A.F. was supported by MRC Grants MR/K001930/1 and MR/N023250/1 and Biotechnology and Biological Sciences Research Council (BBSRC) Grant BB/N002539/1. R.C.D.F. and D.A.I.M. were supported by the MRC Career Development Award MR/M009505/1. D.A.-J. acknowledges support by the MINECO Contract CTQ2016-76941-R, Fundación Biofísica Bizkaia, the Basque Excellence Research Centre (BERC) program and IT709-13 of the Basque Government, and Fundación BBVA. M.A.S.-P. was supported by the MINECO under the "Juan de la Cierva Postdoctoral program" (position FJCI-2015-25725). Technical support from the CIC bioGUNE Metabolomics and Proteomics platforms are gratefully acknowledged.

Author contributions

L.M.N. designed the overall experimental plan for the manuscript, performed the majority of the experiments presented and wrote the manuscript. A.K.C. performed all TraDIS sequencing and associated bioinformatic analyses. T.C. and R.C.D.F. performed pull-down experiments and bacterial growth assays. E.M. assisted with protein pull-down assays. M.A.S.-P. and D.A.-J. performed protein purification and MS enzymatic assays. D.A.-J. performed homology modelling and bioinformatic analyses; G.D. and J.P. contributed to project management and supported TraDIS sequencing and associated bioinformatic analyses. D.A.I.M. contributed to project management, designed experiments, performed protein purification and pull-down experiments, and contributed to the writing of the manuscript. A.F. contributed to project management, designed the overall experimental plan for the manuscript and contributed to writing the manuscript.

Competing interests

The authors declare no competing interests.

Additional information

Extended data is available for this paper at https://doi.org/10.1038/s41564-021-00950-8.

Supplementary information The online version contains supplementary material available at https://doi.org/10.1038/s41564-021-00950-8.

Correspondence and requests for materials should be addressed to D.A.I.M. or A.F.

Peer review information *Nature Microbiology* thanks the anonymous reviewers for their contribution to the peer review of this work. Peer reviewer reports are available.

Reprints and permissions information is available at www.nature.com/reprints.

Publisher's note Springer Nature remains neutral with regard to jurisdictional claims in published maps and institutional affiliations.

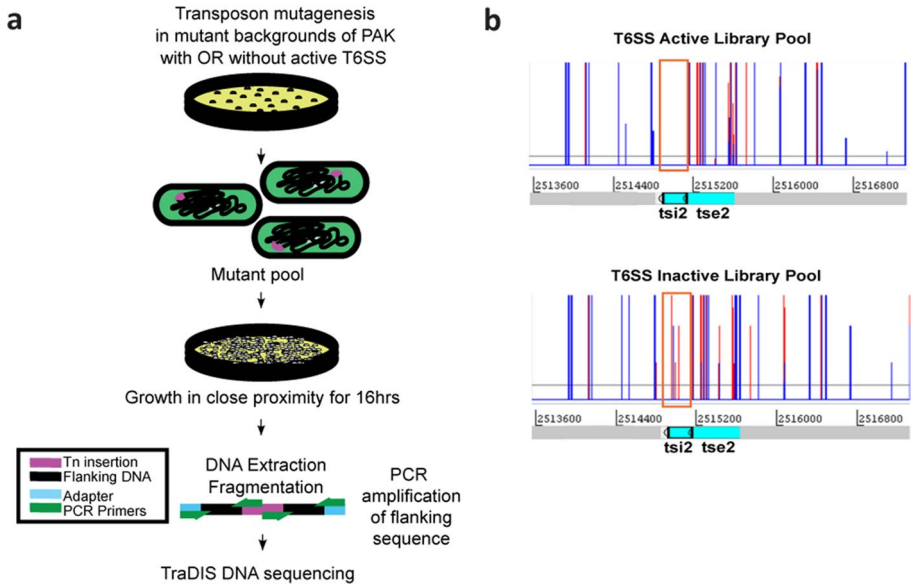

Extended Data Fig. 1 | TraDIS library generation and sequencing workflow and predicted outcome of transposon insertions in *tsi* (immunity) genes in each library background. a, *En masse* transposon (Tn) mutagenesis in T6SS active (PAKΔ*retS*) or T6SS inactive (PAKΔ*retS*ΔH1) backgrounds was performed to generate pooled transposon mutant libraries of ~2 million mutants each. These libraries were then separately passaged overnight at high contact density and the genomic DNA from recovered mutants was harvested. This genomic DNA was then fragmented and adaptors ligated to each end prior to PCR enrichment for transposon-containing DNA fragments. The pooled DNA population was then subjected to TraDIS DNA sequencing. **b**, Artemis (http://www.sanger.ac.uk/science/tools/artemis - version 17/0.1) plot file showing distribution of transposon insertions (red and blue lines correspond to insertions mapped from either forward or reverse sequence reads) in immunity gene (*tsi2* in this case) in the T6SS active library background (top panel - no insertions permitted) and in the T6SS inactive library background (right - insertions are permitted). The other H1-T6SS immunity genes detected, as well as the putative previously unidentified T6SS immunity genes (Table 1) had a similar distribution of transposon insertions in each library background as for *tsi2*. Panel (a) adapted from Barquist *et al*., (2013)[56].

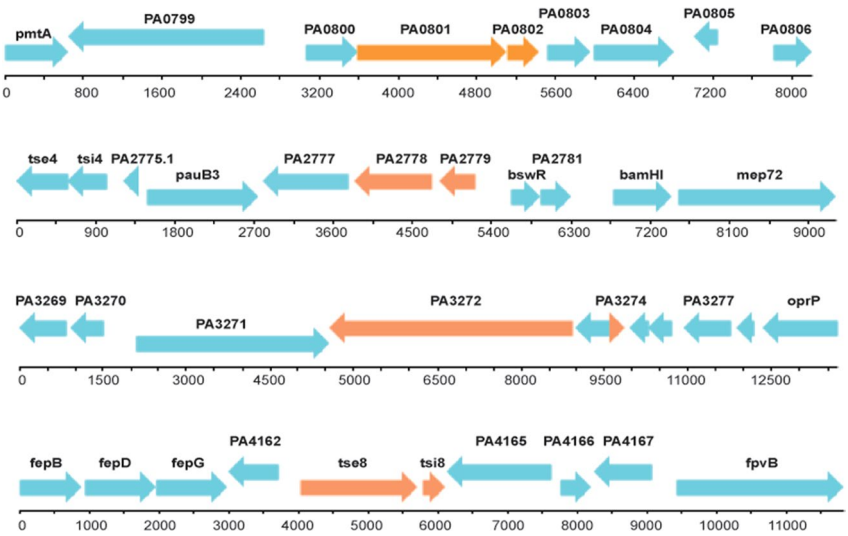

Extended Data Fig. 2 | Genomic context of putative toxin-immunity pairs identified in TraDIS screen. Putative toxin and immunity pairs from Table 1 are in orange with surrounding genes in blue. Genes corresponding to PAO1 ORF numbers. Base pairs covering the region are marked below each gene sequence.

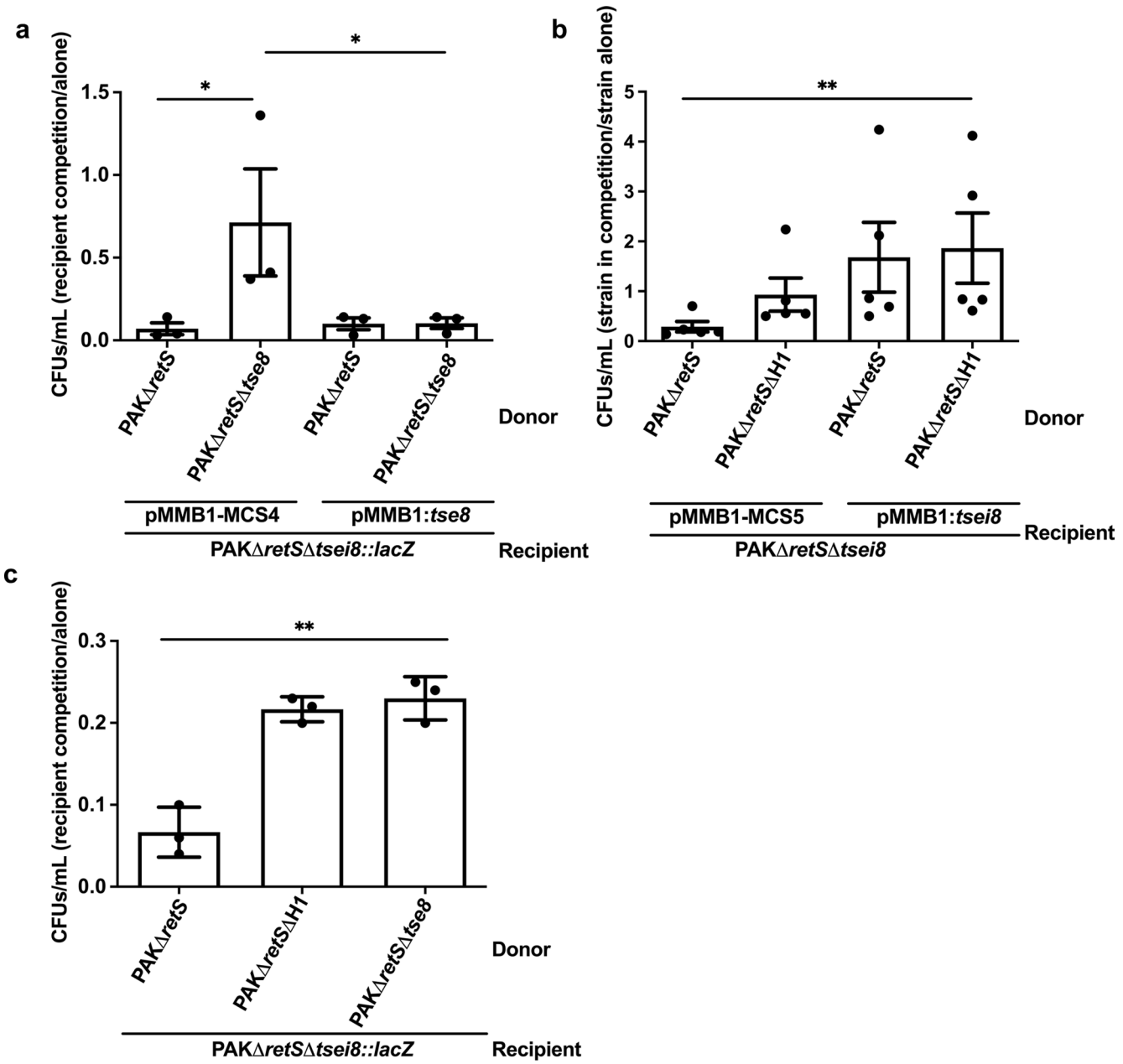

Extended Data Fig. 3 | Prey killing is mediated by Tse8 and effects can be complemented by expressing Tse8 or Tsei8 *in trans*. **a**, In the absence of Tse8 (PAKΔ*retS*Δ*tse8*) or the H1-T6SS (PAKΔ*retS*ΔH1) there is no reduction in recovered recipient (PAKΔ*retS*Δ*tsei8*) as occurs when the donor has a fully active T6SS (PAKΔ*retS*). **b-c**, The PAKΔ*retS*Δ*tsei8* **(b)** or PAKΔ*retS*Δ*tse8* **(c)** mutation can be complemented *in trans*. Competition assays were performed with donors PAKΔ*retS* or PAKΔ*retS*Δ*H1* and recipient PAKΔ*retS*Δ*tsei8* with either empty pBBR1MCS5 or the complementation vector pBBR1:*tsei8* **(b)** or recipient PAKΔ*retS*Δ*tsei8* with either empty pBBR1MCS4 or the complementation vector pBBR1:*tse8* **(c)**. Statistical analyses: **a**, Mean CFUs/mL ± SEM of recipient cells in competition/alone are represented from represented from three independent replicates performed in triplicate (n=3). Two-tailed student's t-test, * $p<0.05$ for PAKΔ*retS* [pBBR1-MCS4] vs recipient compared to PAKΔ*retS*Δ*tse8* [pBBR1-MCS4] vs recipient, PAKΔ*retS*Δ*tse8* [pBBR1-MCS4] vs recipient compared to PAKΔ*retS* [pBBR1:*tse8*] or PAKΔ*retS*Δ*tse8* [pBBR1:*tse8*] vs recipient. **b**, Mean CFUs/mL ± SEM of recipient cells in competition/alone are represented from represented from five independent replicates performed in triplicate (n=5). Two-tailed student's t-test, ** $p<0.005$ compared to PAKΔ*retS* donor vs recipient PAKΔ*retS*Δ*tsei8* [pBBR1-MCS5] compared separately to the other datasets; ns between recovered CFUs/mL for recipient PAKΔ*retS*Δ*tsei8* [pMMB-MCS5] *vs* PAKΔ*retS*ΔH1 ($p=0.51$) and recipient PAKΔ*retS*Δ*tsei8* [pMMB:*tsei8*] *vs* PAKΔ*retS* ($p=0.61$). **c**, Mean CFUs/mL ± SEM of recipient cells in competition/alone are represented from represented from three independent replicates performed in triplicate (n=3). Two-tailed student's t-test, ** $p<0.005$ for PAKΔ*retS* donor vs recipient compared separately to the other datasets.

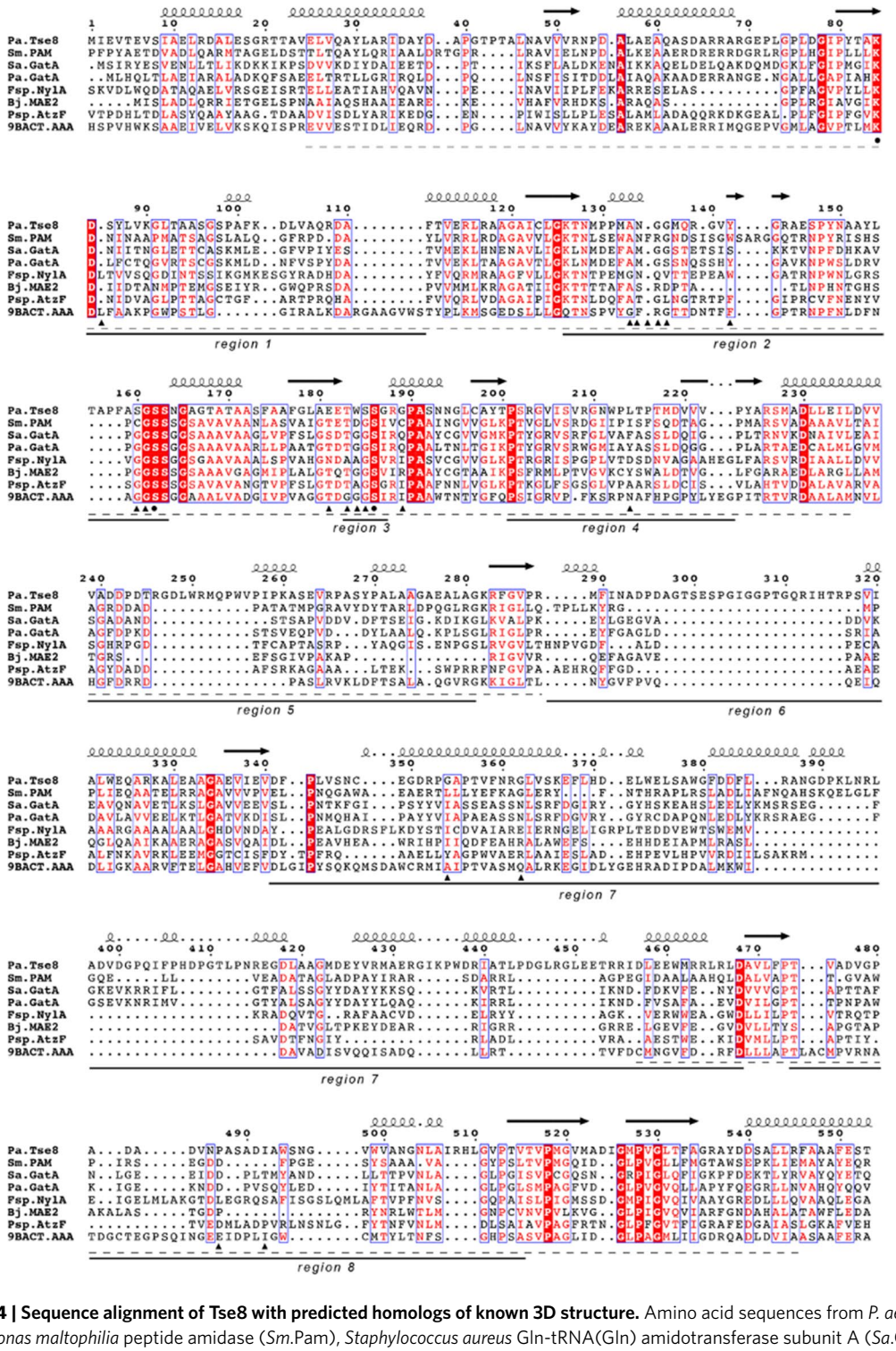

Extended Data Fig. 4 | Sequence alignment of Tse8 with predicted homologs of known 3D structure. Amino acid sequences from *P. aeruginosa* Tse8 (*Pa.* Tse8), *Stenotrophomonas maltophilia* peptide amidase (*Sm.*Pam), *Staphylococcus aureus* Gln-tRNA(Gln) amidotransferase subunit A (*Sa.*GatA), *P. aeruginosa* Asn-tRNA(Asn) transamidosome subunit A (*Pa.*GatA), *Flavobacterium sp.* 6-aminohexanoate cyclic dimer hydrolase NylA (*Fsp.*NylA), *Bradyrhizobium japonicum* malonamidase E2 (*Bj.*MAE2), *Pseudomonas sp.* allophanate hydrolase (*Psp.*AtzF) and *Bacterium csbl00001* Aryl Acylamidase (*9BACT.*AAA) were aligned. Residues are colour-coded depending on the percentage of equivalences; white letter in red background for residue 100 % conserved, red letter in white background for residue with physical-chemical properties conserved. The secondary structure elements found in the 3D structure of *Sm.*PAM are represented above the alignment (black arrows correspond to β-sheets and curly lines to α-helices). The conserved Ser-Ser-Lys catalytic triad is indicated below the alignment by black circles. The AS signature sequence is indicated below the alignment by a dotted line. Regions that protrude out of the core AS domain are numbered below the alignment. Residues found to interact with substrates/substrate analogues, products or inhibitors are indicated with black triangles below the alignment (analysis was carried out for crystal structures with the following PDB codes: 1M21 (*Sm.*Pam), 1O9O (*Bj.*MAE2), 4CP8 (*Psp.*AtzF) and 4YJI (*9BACT.*AAA)). Alignment was generated using MUSCLE[57] and graphical representation was performed with ESPript 3[58].

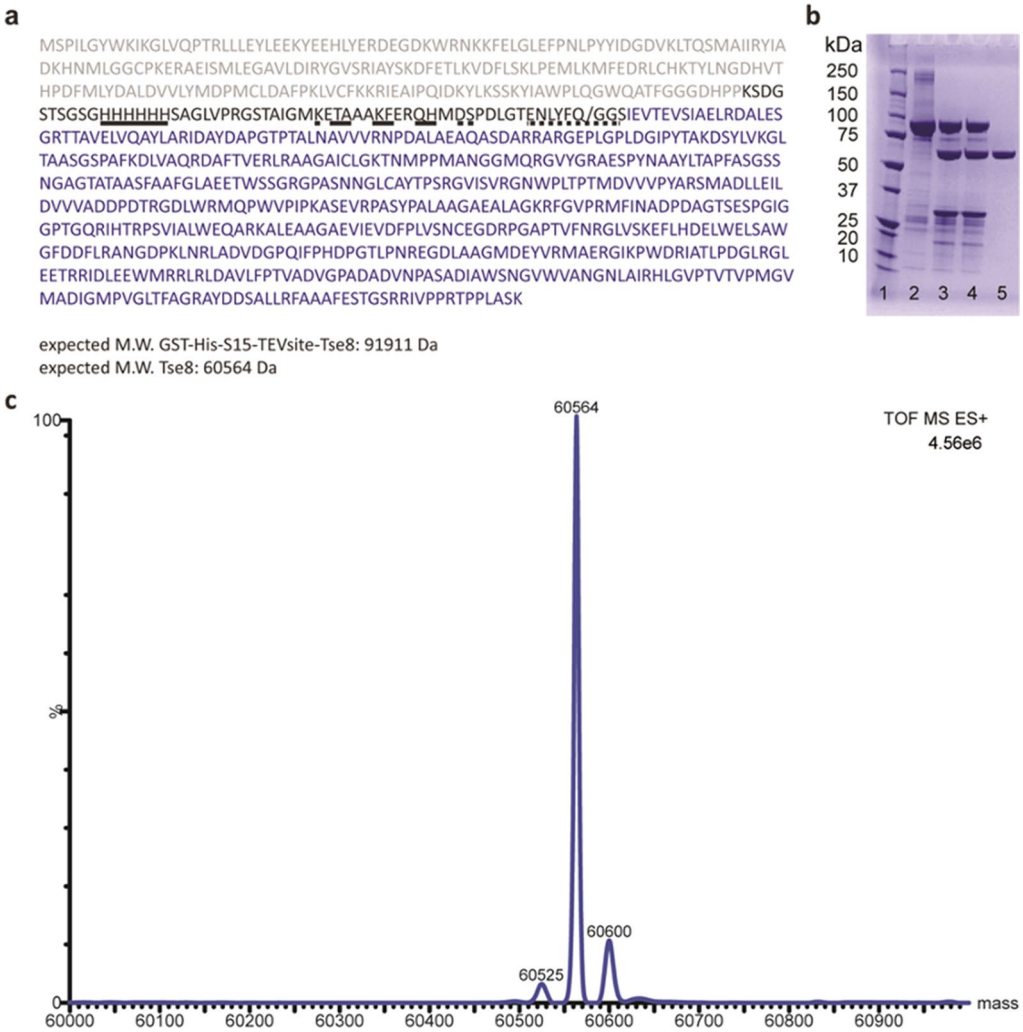

Extended Data Fig. 5 | Recombinant production of Tse8. a, Amino acid sequence of *Pseudomonas aeruginosa* GST-TEV-Tse8 construct. The recombinant Tse8 construct contains a fused glutathione S-transferase (GST) tag (grey colour), a S15 tag (dashed line), a poly-histidine tag (smooth line) and the optimal Tobacco Etch Virus protease (TEV) cleavage site (ENLYFQG) (dotted line) at the N-terminus of Tse8 (in blue letters). **b**, Sodium dodecyl sulfate polyacrylamide gel electrophoresis (SDS-PAGE) of purified Tse8. Lane 1, molecular weight marker; Lane 2, sample before cleaving with TEV; Lanes 3-4, sample after incubation with TEV; Lane 5, Tse8 without tags (4-20% gel (ExpressPlus™ PAGE Gel, GenScript). **c**, Deconvoluted electrospray ionization mass spectrometry (ESI-MS) chromatogram of purified Tse8 after TEV cleavage (the experimentally determined molecular weight corresponds to the expected molecular weight of 60,564 Da). Experiments described in (b) and (c) were performed in one biological replicate.

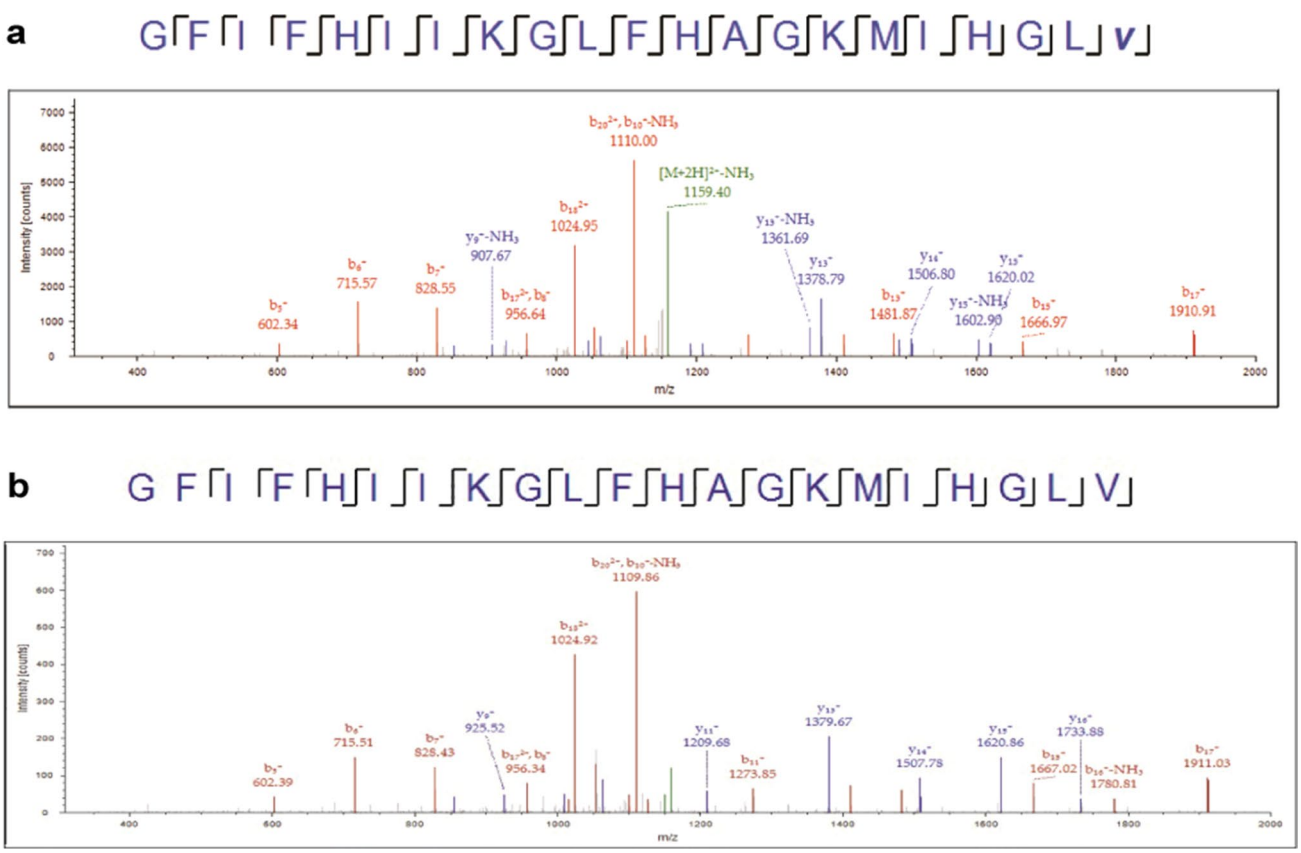

Extended Data Fig. 6 | Tse8 is not active on a substrate of the amidase Pam. MS analysis of Tse8 **(a)** or Pam **(b)** enzymatic assay using epinicedin-1 as substrate. The antimicrobial peptide epinecidin-1, as well as sermorelin, have amidated C termini. The latter has previously been used to measure the amidase activity of Pam from *S. maltophilia*[55]. In both **(a)** and **(b)**: Sequence covered by the fragments obtained after fragmentation of epinecidin-1 in the MS is indicated above the fragmentation spectra for epinecidin-1. Signals corresponding to the amidated **(a)** or deamidated **(b)** form of epinecidin-1 are shown in the spectral plot with red ions belonging to the *b* series of fragments, blue ions to the *y* series, and green ions to parental forms of the peptide. See Extended Data Fig. 7 for correspondence between the observed fragments and their theoretical masses.

a

#1	b^+	b^{2+}	Seq.	y^+	y^{2+}	#2
1	58.02875	29.51801	G			21
2	205.09717	103.05222	F	2277.32063	1139.16395	20
3	318.18124	159.59426	I	2130.25221	1065.62974	19
4	465.24956	233.12847	F	2017.16814	1009.08771	18
5	602.30857	301.65792	H	1870.00997	935.5535	17
6	715.39264	358.19996	I	1733.04081	867.02404	16
7	828.47671	414.74199	I	1619.95674	810.48201	15
8	956.57168	478.78948	K	1506.87267	753.93997	14
9	1013.59315	507.30021	G	1387.7777	689.89249	13
10	1126.67722	563.84225	L	1321.75623	661.38175	12
11	1273.74564	637.37646	F	1208.67216	604.83972	11
12	1410.80455	705.90591	H	1061.60374	531.30551	10
13	1481.84167	741.42447	A	924.54483	462.77605	9
14	1538.86314	769.93521	G	853.50771	427.25749	8
15	1666.95811	833.98269	K	796.48624	398.74676	7
16	1797.99861	899.50294	M	668.39127	334.69927	6
17	1911.08268	956.04498	I	537.35077	269.17902	5
18	2048.14159	1024.57443	H	424.2667	212.63699	4
19	2105.16306	1053.08517	G	287.20779	144.10753	3
20	2218.24713	1109.6272	L	230.18632	115.5668	2
21			V-Amidated	117.10225	59.05476	1

#1	b-NH_3^+	b-NH_3^{2+}	Seq.	y-NH_3^+	b-NH_3^{2+}	#2
1			G			21
2			F	2260.29408	1130.65068	20
3			I	2113.22566	1057.11647	19
4			F	2000.14159	1000.57443	18
5			H	1853.07317	927.04022	17
6			I	1716.01426	858.51077	16
7			I	1602.93019	745.4267	15
8	939.54513	470.2762	K	1489.84612	681.37921	14
9	996.5666	498.78594	G	1364.75115	652.86848	13
10	1109.65067	555.32897	L	1304.72968	596.32644	12
11	1265.71909	628.86318	F	1191.64561	522.79223	11
12	1393.778	697.39264	H	1044.57719	454.26278	10
13	1464.81512	732.9112	A	907.51828	418.74422	9
14	1521.83659	761.42193	G	836.48113	390.23348	8
15	1649.93156	825.56942	K	779.45969		7
16	1780.97206	890.98967	M			6
17	1894.05613	947.5317	I			5
18	2031.11504	1016.06116	H			4
19	2088.13651	1044.57189	G			3
20	2201.22058	1101.11393	L			2
21			V-Amidated			1

Precursors	Values
$[M + 2H]^{2+}$-H_2O-NH_3	1148.68011
$[M + 2H]^{2+}$-NH_3	1157.6694
$[M + 2H]^{2+}$-H_2O	1157.68539
$[M + 2H]^{2+}$	1168.67469

b

#1	b^+	b^{2+}	Seq.	y^+	y^{2+}	#2
1	58.02875	29.51801	G			21
2	205.09717	103.05222	F	2278.30464	1139.16395	20
3	318.18124	159.59426	I	2131.23622	1065.62974	19
4	465.24956	233.12847	F	2018.15215	1009.08771	18
5	602.30857	301.65792	H	1871.08373	935.5535	17
6	715.39264	358.19996	I	1734.02482	867.02404	16
7	828.47671	414.74199	I	1620.94075	810.48201	15
8	956.57168	478.78948	K	1507.85668	753.93997	14
9	1013.59315	507.30021	G	1379.76171	689.89249	13
10	1126.67722	563.84225	L	1322.74024	661.38175	12
11	1273.74564	637.37646	F	1209.62617	604.83972	11
12	1410.80455	705.90591	H	1062.58775	531.30551	10
13	1481.84167	741.42447	A	925.52884	462.77605	9
14	1538.86314	769.93521	G	854.49172	427.25749	8
15	1666.95811	833.98269	K	797.47025	398.74676	7
16	1797.99861	899.50294	M	669.38528	334.69927	6
17	1911.08268	956.04498	I	538.33478	269.17902	5
18	2048.14159	1024.57443	H	425.25071	212.63699	4
19	2105.16306	1053.08517	G	288.1918	144.10753	3
20	2218.24713	1109.6272	L	231.17033	115.5668	2
21			V	118.08626	59.05476	1

#1	b-NH_3^+	b-NH_3^{2+}	Seq.	y-NH_3^+	b-NH_3^{2+}	#2
1			G			21
2			F	2261.27809	1131.14268	20
3			I	2114.20967	1057.60847	19
4			F	2001.1256	1001.06644	18
5			H	1854.05718	927.53223	17
6			I	1706.99827	859.00277	16
7			I	1603.9142	802.46074	15
8	939.54513	470.2762	K	1490.83013	745.9187	14
9	996.5666	498.78594	G	1362.73516	681.87122	13
10	1109.65067	555.32897	L	1305.71369	653.36048	12
11	1265.71909	628.86318	F	1192.62962	596.81845	11
12	1393.778	697.39264	H	1045.5612	523.28424	10
13	1464.81512	732.9112	A	908.50229	454.75478	9
14	1521.83659	761.42193	G	837.46517	419.23622	8
15	1649.93156	825.56942	K	780.4437	390.72549	7
16	1780.97206	890.98967	M			6
17	1894.05613	947.5317	I			5
18	2031.11504	1016.06116	H			4
19	2088.13651	1044.57189	G			3
20	2201.22058	1101.11393	L			2
21			V			1

Precursors	Values
$[M + 2H]^{2+}$-H_2O-NH_3	1150.64814
$[M + 2H]^{2+}$-NH_3	1159.65342
$[M + 2H]^{2+}$-H_2O	1159.16141
$[M + 2H]^{2+}$	1168.16669

Extended Data Fig. 7 | Theoretical masses for the fragments detected during MS analysis of the amidase reactions presented in Extended Data Fig. 6. In both **(a)** and **(b)**: Correspondence between the observed fragments and their theoretical masses. Tables correspond to unaltered ion series at +1 and +2 charge states (left), ion series after neutral losses at +1 and +2 charge states (ammonia loss, centre) and parental ion masses at +2 charge state with or without diverse neutral losses (right). Red ions belong to the *b* series of fragments, blue ions to the *y* series, and green ions to parental forms of the peptide. See Extended Data Fig. 6 for corresponding spectral plots.

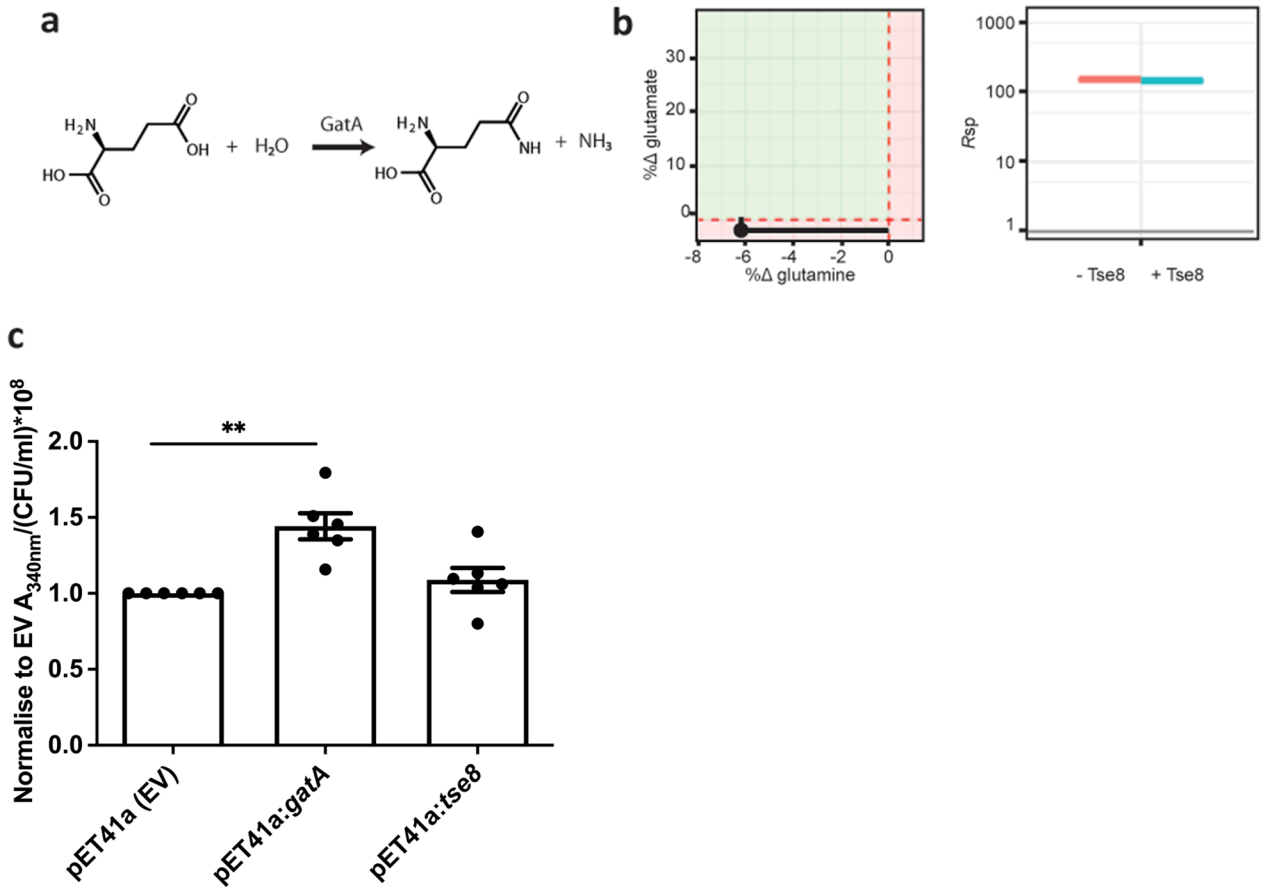

Extended Data Fig. 8 | Tse8 is not active on a substrate of GatA. a, Amidase reaction catalysed by GatA and **b**, MS analysis of Tse8 enzymatic assay using glutamine as substrate. Signal of the expected product (glutamate) was also found as a contaminant in the blank and product stock and therefore subtracted from the reaction incubation. The graph on the left shows relative differences (%Δ) of glutamate and glutamine in reaction incubation and blank samples. The green-shaded area indicates the zone in which the observed differences could indicate enzymatic reaction. ($\%\Delta_{Product}$ = 100 * ([product in incubation] – [product in blank]/ [product in incubation]; $\%\Delta_{Substrate}$ = 100 * ([substrate in incubation] – [substrate in blank]/ [substrate in incubation]). The graph on the right shows the ratios between substrate and product (R_{sp}) in the blank (red) and reaction (Tse8) incubation (blue) samples. The product signal (contaminant) was *ca.* 100 times lower than that of the substrate. (R_{sp} = (Signal substrate / Signal product)). **c**, Glutaminase assays of lysates of *E. coli* cells expressing GatA, Tse8 or empty vector demonstrate that Tse8 does not have the same substrate (L-glutamine) as GatA as measured by relative NADPH levels/(CFU/mLx10^8) and here normalized to empty vector (EV) mean. Mean ± SEM of six biological replicates performed in triplicate (n=6). Two-tailed student's t-test, ** p<0.005 for empty vector compared to pET41a:*gatA*; ns for empty vector compared to pET41A:*tse8* (p=0.621).

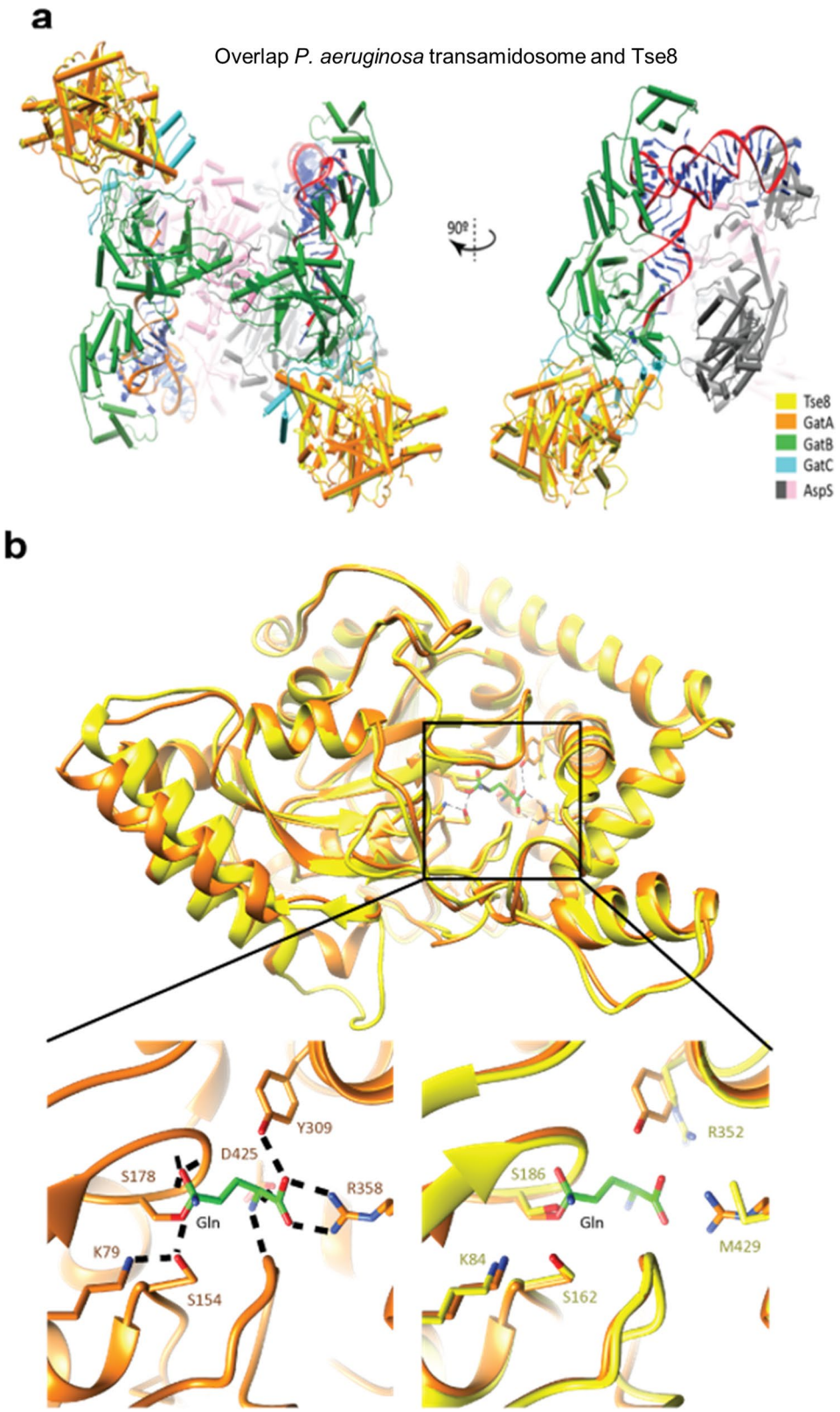

Extended Data Fig. 9 | Tse8 is structurally similar to GatA of the transamidosome complex. a, Structure of the *P. aeruginosa* GatCAB transamidosome-Asp-tRNA structure (PDB: 4WJ3). **b**, Top panel: Tse8 3D homology model generated using GatA from *S. aureus* (from PDB: 2F2A) as template overlaid with the A subunit of the solved GatCAB transamidosome-AspS-tRNA structure from *P. aeruginosa* (PDB: 4WJ3). The reaction centre with covalently bound glutamine substrate is boxed. Bottom panel: Close-up view of the reaction centre of *S. aureus* GatA (left) with glutamine (green) substrate bound and of a superposition of *S. aureus* GatA and the 3D homology model of *P. aeruginosa* Tse8 (right) showing the predicted conservation of the Ser-*cis*Ser-Lys catalytic triad and predicted divergent substrate binding residues in Tse8 compared to GatA.

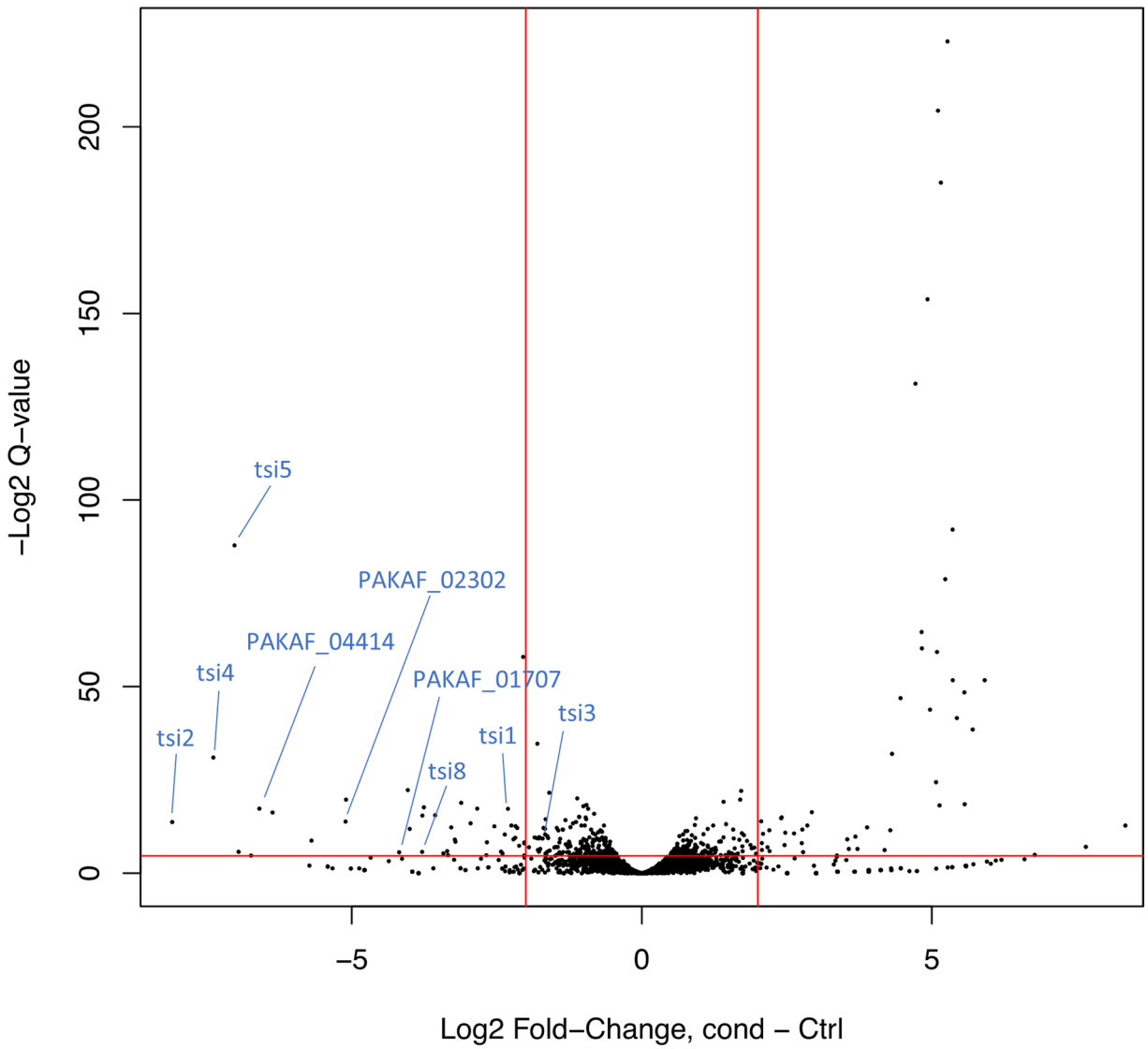

Extended Data Fig. 10 | Volcano plot showing the spread of changes in abundance of TraDIS mutants for each *P. aeruginosa* gene during T6SS active compared to inactive conditions. Each black dot represents the comparative fold change of insertions for each gene. Red lines show the cut-off criteria of 5% false discovery rate (horizontal) and a $\log_2$ fold change (Log_2FC) of 2 (vertical). The corresponding Log2 Fold-Change values on the x-axis for each gene are reported Supplementary Table 1. A -Log2 transformation has been applied to the corresponding Q-values for each gene as reported in Supplementary Table 1. Immunity genes and putative immunity genes (as shown in Table 1) are shown in blue.

nature research

Corresponding author(s): NMICROBIOL-18061103-T

Corresponding authors Alalain Filloux (a.filloux@imperial.ac.uk
Despoina A.I. Mavridou (despoina.mavridou@austin.utexas.edu)

Reporting Summary

Nature Research wishes to improve the reproducibility of the work that we publish. This form provides structure for consistency and transparency in reporting. For further information on Nature Research policies, see Authors & Referees and the Editorial Policy Checklist.

Statistical parameters

When statistical analyses are reported, confirm that the following items are present in the relevant location (e.g. figure legend, table legend, main text, or Methods section).

n/a	Confirmed	
☐	☒	The exact sample size (*n*) for each experimental group/condition, given as a discrete number and unit of measurement
☐	☒	An indication of whether measurements were taken from distinct samples or whether the same sample was measured repeatedly
☐	☒	The statistical test(s) used AND whether they are one- or two-sided *Only common tests should be described solely by name; describe more complex techniques in the Methods section.*
☒	☐	A description of all covariates tested
☒	☐	A description of any assumptions or corrections, such as tests of normality and adjustment for multiple comparisons
☐	☒	A full description of the statistics including central tendency (e.g. means) or other basic estimates (e.g. regression coefficient) AND variation (e.g. standard deviation) or associated estimates of uncertainty (e.g. confidence intervals)
☐	☒	For null hypothesis testing, the test statistic (e.g. *F*, *t*, *r*) with confidence intervals, effect sizes, degrees of freedom and *P* value noted *Give P values as exact values whenever suitable.*
☒	☐	For Bayesian analysis, information on the choice of priors and Markov chain Monte Carlo settings
☒	☐	For hierarchical and complex designs, identification of the appropriate level for tests and full reporting of outcomes
☒	☐	Estimates of effect sizes (e.g. Cohen's *d*, Pearson's *r*), indicating how they were calculated
☐	☒	Clearly defined error bars *State explicitly what error bars represent (e.g. SD, SE, CI)*

Our web collection on statistics for biologists may be useful.

Software and code

Policy information about availability of computer code

Data collection	No software used
Data analysis	EdgeR version 3.10.5 - https://bioconductor.org/packages/release/bioc/html/edgeR.html; MUSCLE version 3.8.31 - https://www.ebi.ac.uk/Tools/msa/muscle/; ENDscript server version 2.0.7 - https://endscript.ibcp.fr/ESPript/ENDscript/; Image J version 1.51 - https://imagej.nih.gov/ij/download.html; BLAST version 2.7.1 - https://blast.ncbi.nlm.nih.gov/Blast.cgi; FASTA version 36.3.8f - https://www.ebi.ac.uk/Tools/sss/fasta/; Uniprot/Swissprot version 2018_10 - https://www.uniprot.org/; Artemis 17.0.1 Wellcome Trust Sanger Institute, Cambridge UK - http://www.sanger.ac.uk/science/tools/artemis

For manuscripts utilizing custom algorithms or software that are central to the research but not yet described in published literature, software must be made available to editors/reviewers upon request. We strongly encourage code deposition in a community repository (e.g. GitHub). See the Nature Research guidelines for submitting code & software for further information.

Data

Policy information about availability of data

All manuscripts must include a data availability statement. This statement should provide the following information, where applicable:

- Accession codes, unique identifiers, or web links for publicly available datasets
- A list of figures that have associated raw data
- A description of any restrictions on data availability

PAK genome NCBI number is LR657304 and in the ENA (European Nucleotide Archive) is ERS195106 (https://www.ebi.ac.uk/ena/browser/view/ERS195106). The resulting sequences of the T6SS TraDIS assays are available from the ENA under study accession number ERS577921 (https://www.ebi.ac.uk/ena/browser/view/ERS577921).

Field-specific reporting

Please select the best fit for your research. If you are not sure, read the appropriate sections before making your selection.

☒ Life sciences ☐ Behavioural & social sciences ☐ Ecological, evolutionary & environmental sciences

For a reference copy of the document with all sections, see nature.com/authors/policies/ReportingSummary-flat.pdf

Life sciences study design

All studies must disclose on these points even when the disclosure is negative.

Sample size	This is not applicable for this study. Experiments were conducted at least in biological triplicate (where needed), no experimental data was excluded, and all attempts for replication were successful.
Data exclusions	No data were excluded.
Replication	Experiments were conducted in at least biological triplicate and appropriate tests performed to determine statistical significance of the data. All attempts at replication were successful.
Randomization	This is not relevant to this study as we did not perform sampling. Where applicable, experiments were performed in at least biological triplicate, each performed on a different day to account for day-to-day variations.
Blinding	Blinding was not performed in this study. All data relied upon quantitative outputs which as such were not open to subjective bias in interpretation of the results.

Reporting for specific materials, systems and methods

Materials & experimental systems

n/a	Involved in the study
☐	☒ Unique biological materials
☐	☒ Antibodies
☒	☐ Eukaryotic cell lines
☒	☐ Palaeontology
☒	☐ Animals and other organisms
☒	☐ Human research participants

Methods

n/a	Involved in the study
☒	☐ ChIP-seq
☒	☐ Flow cytometry
☒	☐ MRI-based neuroimaging

Unique biological materials

Policy information about availability of materials

Obtaining unique materials	The only unique materials generated in this study are bacterial strains and plasmids. All inquiries about these should be directed to and will be fulfilled by the Lead Contact, Alain Filloux (alain.filloux@imperial.ac.uk)

Antibodies

Antibodies used	Monoclonal anti-His tag antibody produced in mouse Sigma SAB1305538; Anti-HA.11 tag antibody produced in mouse Biolegend MMS-101R; Monoclonal anti-V5 tag antibody produced in mouse Invitrogen R960-25

Strep-Tactin HRP conjugate IBA-lifesciences 2-1502-001; Secondary antibody goat anti-mouse IgG HRP conjugate Sigma 12-349

Validation

anti-His antibody validation: https://www.sigmaaldrich.com/catalog/product/sigma/sab1305538?lang=en&region=GB
anti-HA antibody validation: https://www.biolegend.com/en-us/products/anti-ha-11-epitope-tag-antibody-11071
anti-V5 antibody validation: https://www.thermofisher.com/antibody/product/V5-Tag-Antibody-Monoclonal/R960-25
Goat anti-mouse IgG HRP conjugate validation: https://www.merckmillipore.com/GB/en/product/Goat-Anti-Mouse-IgG-Antibody-HRP-conjugate,MM_NF-12-349?bd=1#anchor_COA
Strep-Tactin HRP conjugate validation:
https://www.iba-lifesciences.com/media/17/bf/a6/1623836391/DS_2-1502_ST-HRP-conj.pdf